Clim. Past, 21, 2031–2060, 2025
https://doi.org/10.5194/cp-21-2031-2025
© Author(s) 2025. This work is distributed under
the Creative Commons Attribution 4.0 License.

Climate of the Past
Open Access
EGU

Holocene land cover change in North America: continental trends, regional drivers, and implications for vegetation–atmosphere feedbacks

Andria Dawson[1,15,★], John W. Williams[2,★], Marie-José Gaillard[3], Simon J. Goring[2], Behnaz Pirzamanbein[4], Johan Lindstrom[5], R. Scott Anderson[6], Andrea Brunelle[7], David Foster[8], Konrad Gajewski[9], Daniel G. Gavin[10], Terri Lacourse[11], Thomas A. Minckley[12], Wyatt Oswald[13], Bryan Shuman[12], and Cathy Whitlock[14]

[1]Department of Mathematics and Computing, Calgary, AB, T3E6K6, Canada
[2]Department of Geography and Center for Climatic Research, University of Wisconsin-Madison, Madison, WI 53706, USA
[3]Department of Biology and Environmental Science, Linnaeus University, E 39231 Kalmar, Sweden
[4]Department of Statistics, School of Economics and Management, Lund University, 220 07 Lund, Sweden
[5]Division of Mathematical Statistics, Centre for Mathematical Sciences, Lund University, 221 00 Lund, Sweden
[6]School of Earth and Sustainability, Northern Arizona University, Flagstaff, AZ 86011, USA
[7]Geography Department, University of Utah, Salt Lake City, UT 84112, USA
[8]Harvard Forest, Harvard University, Petersham, MA 01366, USA
[9]Département de Géographie, Environnement et Géomatique, Université d'Ottawa, Ottawa, ON K1N 6N50, Canada
[10]Department of Geography, University of Oregon, Eugene, OR 97403, USA
[11]Department of Biology and Centre for Forest Biology, University of Victoria, Victoria, BC V8P 5C2, Canada
[12]Department of Geology and Geophysics, University of Wyoming, Laramie, WY 82071, USA
[13]Marlboro Institute for Liberal Arts and Interdisciplinary Studies, Emerson College, Boston, MA 02116 , USA
[14]Department of Earth Sciences, Montana State University, Bozeman, MT 59717, USA
[15]Department of Biology, Mount Royal University, Calgary, AB, T3E6K6, Canada
★These authors contributed equally to this work.

Correspondence: Andria Dawson (adawson@mtroyal.ca)

Received: 30 January 2024 – Discussion started: 20 February 2024
Revised: 29 November 2024 – Accepted: 20 January 2025 – Published: 6 November 2025

Abstract. Land cover governs the biogeophysical and biogeochemical feedbacks between the land surface and atmosphere. Holocene vegetation–atmosphere interactions are of particular interest, both to understand the climate effects of intensifying human land use and as a possible explanation for the Holocene temperature conundrum, a widely studied mismatch between simulated and reconstructed temperatures. Progress has been limited by a lack of data-constrained, quantified, and consistently produced reconstructions of Holocene land cover change. As a contribution to the Past Global Changes (PAGES) LandCover6k Working Group, we present a new suite of land cover reconstructions with uncertainty for North America, based on a network of 1445 sedimentary pollen records and the REVEALS pollen–vegetation model (PVM) coupled with a Bayesian spatial model. These spatially comprehensive land cover maps are then used to determine the pattern and magnitude of North American land cover changes at continental to regional scales. Early Holocene afforestation in North America was driven by rising temperatures and deglaciation, and this afforestation likely amplified early Holocene warming via the albedo effect. A continental-scale mid-Holocene peak in summergreen trees and shrubs (8.5 to 4 ka) is hypothesized to represent a positive and understudied feedback loop among insolation, temperature, and phenology. A last-millennium decrease in summergreen trees and shrubs with corresponding increases in open land was likely driven by a spatially varying combination of intensifying land use

and neoglacial cooling. Land cover trends vary within and across regions, due to individualistic taxon-level responses to environmental change. Major species-level events, such as the mid-Holocene decline in *Tsuga canadensis* (eastern hemlock), may have altered regional climates. The substantial land cover changes reconstructed here support the importance of biogeophysical and biogeochemical vegetation feedbacks to Holocene climate–carbon dynamics. However, recent model experiments that invoke vegetation feedbacks to explain the Holocene temperature conundrum may have overestimated land cover forcing by replacing Northern Hemisphere grasslands $> 30°$ N with forests, an ecosystem state that is not supported by these land cover reconstructions. These Holocene reconstructions for North America, along with similar LandCover6k products now available for other continents, serve the Earth system modeling community by providing better-constrained land cover scenarios and benchmarks for model evaluation, ultimately making it possible to better understand the regional- to global-scale processes driving Holocene land cover, carbon cycle, and climate dynamics.

1 Introduction

Vegetation is the great mediator of biogeophysical and biogeochemical interactions between the land surface and the atmosphere (Bonan and Doney, 2018; Gaillard et al., 2010; Harrison et al., 2020; Pongratz et al., 2010). Enhanced carbon uptake and sequestration by terrestrial ecosystems is an essential component to contemporary net-negative CO_2 emission scenarios needed to stabilize the climate system and mitigate the dangerous impacts already emerging (Rogelj et al., 2018; van Vuuren et al., 2017). During the Holocene, as cryosphere–ocean–atmosphere feedbacks waned and anthropogenic land use intensified (Ruddiman, 2013; Stephens et al., 2019), vegetation–atmosphere feedbacks and forcings increased in importance, particularly in regions where climate variability interacted with major changes in vegetation structure (Foley et al., 1994). Examples include soil and vegetation feedbacks that amplified precessional-driven variations in monsoonal rainfall intensity in northern Africa and Asia (Chen et al., 2021; Chandan and Peltier, 2020) and increases in high-latitude tree cover, which decreased wintertime albedo and increased temperatures. Carbon sequestration due to Northern Hemisphere postglacial afforestation is estimated at 13.9 GtC between 9 and 6 ka and a 3.5 GtC loss after 3 ka. Intensified human land use and resulting greenhouse gas emissions may have delayed Northern Hemisphere late Holocene cooling and glaciation (Ruddiman, 2003). However, initial models of global anthropogenic land cover change (ALCC) (Kaplan et al., 2009; Klein Goldewijk et al., 2011, 2010) over the Holocene were largely unconstrained by paleoecological and archeological observations and so differed widely in their estimated size and scope of the anthropogenic footprint. More recently, Holocene increases in vegetation cover have been invoked to explain the Holocene temperature conundrum, a discrepancy between proxy and model-estimated temperature during the early to mid-Holocene (Thompson et al., 2022; Kaufman and Broadman, 2023). At subcontinental scales, data-constrained studies of Holocene climate–vegetation feedbacks in Europe indicate that mid-Holocene vegetation changes relative to preindustrial baselines could have warmed winters in some areas by 4–6 °C in northeastern Europe (Strandberg et al., 2022, 2014). Global simulations of vegetation–climate feedbacks during the Holocene, however, remain unconstrained by observational data.

Hence, comprehensive and accurate proxy-based reconstructions of past land cover at regional to global extents are needed (Gaillard and LandCover6k Steering Group, 2015; Gaillard et al., 2018, 2010). These reconstructions can be used with Earth system models (ESMs) to test hypotheses about the physical, biological, and anthropogenic processes that drove Holocene climate variability (Harrison et al., 2020). Fossil pollen records offer the primary observational constraint on past vegetation composition and structure, with thousands of records now available globally. Efforts to systematically map late Quaternary land cover using fossil pollen data and well-defined rule sets began in the late 1990s with the Biome6000 project (Prentice et al., 2000, 2011). Since then, the continental-scale pollen databases launched in the 1980s and 1990s (Grimm et al., 2013) have coalesced along with other paleoecological data into the Neotoma Paleoecology Database (Neotoma), an international, multi-proxy, curated data resource that helps tame issues of data heterogeneity through community curation by experts (Williams et al., 2018). Neotoma thus enables global-scale analyses of past vegetation and climate change (Mottl et al., 2021; Herzschuh et al., 2023).

Multiple pollen–vegetation models (PVMs) have been developed to make quantitative inferences about past vegetation. Some PVMs involve relatively simple but effective transfer functions, such as the modern analogue technique (Williams et al., 2011b) or rule-based systems for classifying land cover (Prentice et al., 2000; Cruz-Silva et al., 2022; Fyfe et al., 2010). Others are process-based proxy system models (Evans et al., 2013) that attempt to represent the processes governing the atmospheric transport and deposition of pollen, such as the REVEALS and LOVE (Sugita, 2007a, b) or STEPPS (Dawson et al., 2019). Efforts continue to test and refine the parameterizations of these models through paired analyses of pollen assemblages and forest composition at local to landscape scales (Liu et al., 2022).

In response to these scientific needs and opportunities, the Past Global Changes (PAGES) LandCover6k Working Group was launched as an international effort (Gaillard and LandCover6k Steering Group, 2015) to reconstruct vegetation globally for the Holocene. LandCover6k, led by experts

typically working at continental scales, has the explicit aim of creating vegetation reconstructions that can better constrain past land use histories in ESMs and is mostly based on networks of fossil pollen records. To facilitate the use of these vegetation reconstructions in ESMs, the REVEALS PVM has been used for all LandCover6k reconstructions, with standard model parameterizations and standard protocols for pollen data handling. LandCover6k gridded REVEALS reconstructions at the continental scale have been published for Europe (Githumbi et al., 2022a, b; Serge et al., 2023; Trondman et al., 2015) and China (Li et al., 2023) so far. However, no comparable REVEALS-based land cover reconstructions are available for North America, despite a comparable density of fossil pollen records to these other regions (Stegner and Spanbauer, 2023) and prior regional-scale applications of REVEALS in North America (Sugita et al., 2010; Chaput and Gajewski, 2018).

REVEALS uses pollen counts, pollen productivity estimates, pollen fall speeds, atmospheric conditions, and sedimentary basin type and size to estimate vegetation composition for a given time period. REVEALS accounts for the processes of differential pollen production (determined by pollen productivity estimates) and dispersal–deposition (determined by the pollen fall speeds, atmospheric conditions, and sedimentary basin type and size).

While REVEALS reconstructions usually combine information from multiple pollen records, the model is not explicitly spatial, so it does not support the interpolation of inferences to places with no pollen records. To address this issue, researchers have developed a statistical approach to spatially interpolate REVEALS-based land cover estimates from individual grid cells to all cells within the grid, including estimates of uncertainty (Pirzamanbein et al., 2014, 2018). The approach uses a Bayesian hierarchical model with spatial dependence specified according to a Gaussian Markov random field (GMRF; Lindgren et al., 2011); we refer to the two-step process of REVEALS-based estimation followed by this spatial interpolation as the REVEALS-GMRF approach. REVEALS-GMRF has been used to develop spatially continuous gridded vegetation reconstructions in Europe to assess vegetation–climate feedbacks resulting from natural and anthropogenic land cover change (Strandberg et al., 2022) and to evaluate ALCC models (Kaplan et al., 2017) and dynamic vegetation models (Pirzamanbein et al., 2020; Dallmeyer et al., 2023; Zapolska et al., 2023).

Here we adopt the REVEALS-GMRF approach to reconstruct land cover changes in North America during the Holocene. This work relies on 1445 Holocene pollen records drawn from Neotoma and its constituent database, the North American Pollen Database (NAPD), with a targeted data mobilization campaign employed to add more records to the NAPD for western North America. Using these data, we reconstruct the fractional cover of 32 plant taxa and three land cover types (LCTs): evergreen trees and shrubs (ETS), summergreen trees and shrubs (STS), and open vegetation/land (OVL; including grasses, herbs, and low shrubs) from 12 000 years ago (12 ka) to the present. We present the Holocene vegetation reconstructions by working across scales, first describing continental-scale trends in land cover, then shifting to several regional-scale case studies to show how the continental-scale trends emerge from taxon-level dynamics that vary within and among regions, with respect to key taxa, drivers, and resultant land cover changes. We then zoom out to discuss the continental-scale drivers of Holocene land cover change in North America and possible biophysical implications of these changes for Holocene vegetation–atmosphere interactions and the Holocene temperature conundrum. Lastly, we discuss the potential limitations of the REVEALS-GMRF approach and the opportunities now available for well-constrained hemispheric- to global-scale studies of vegetation–atmosphere interactions.

2 Data and methods

2.1 Pollen data and data mobilization for western North America

Western North America has traditionally been underrepresented in the NAPD and Neotoma, but the density of fossil pollen records in western North America has steadily increased in recent decades, as multiple teams have worked to collect new records, often focusing on interactions among past vegetation, fire, climate, and human dynamics (Anderson et al., 2008; Gavin and Brubaker, 2014; Marlon et al., 2012; Iglesias et al., 2018; Alt et al., 2018). Many of these datasets were contributed to Neotoma (Williams et al., 2018) when originally published, while others were contributed to Neotoma for an open-data mobilization campaign conducted for this paper and PAGES LandCover6k (Gaillard et al., 2018).

After this effort, 1582 North American Holocene pollen records were downloaded from Neotoma (Supplement Table S1). Each record included pollen count data at a series of depths. For methodological consistency (Flantua et al., 2023), we used the Bayesian age–depth model Bchron to refit all age–depth models using a custom-built workflow (https://github.com/andydawson/bulk-bchron, last access: 25 October 2024). This workflow assessed chronological constraints and used them and IntCal20NH (Reimer et al., 2020) to fit the Bchron age–depth model (Parnell et al., 2008). This resulted in 1445 records with age–depth models. Ages of the youngest and oldest chronological constraints were used to determine the reliable age range for each record; we limited extrapolation of pollen sample ages beyond the youngest or oldest constraints to 1000 years. For discussion, evaluation, and comparison of widely used age–depth models, we refer readers to Lacourse and Gajewski (2020), McKay et al. (2021), and Trachsel and Telford (2017).

Finally, pollen types were aggregated to taxa using the taxa list in the North American Modern Pollen Database (Whit-

more et al., 2005). This resulted in a list of 47 taxa. We identified the taxa that were most abundant and also indicators of land cover type, of which there were 33 (Table S2). There were corresponding pollen productivity and fall speed values for all of these taxa. Among the set of excluded taxa (*Nyssa*, *Platanus*, *Apiaceae*, *Liquidambar*, *Ephedra*, *Cornus*, *Chrysolepis*, *Eriogonum*, *Cactaceae*, *Taxus*, *Larrea*), the fraction of taxon pollen grains with respect to total pollen grain count was at most 0.16 % (*Nyssa*), while the total fraction of excluded pollen taxa was about 0.5 % (for the North American Holocene).

2.2 REVEALS (regional reconstructions)

Pollen-based land cover reconstructions were performed using the REVEALS pollen–vegetation model (Sugita, 2007a) and based on the standard protocol for PAGES LandCover6k (Trondman et al., 2015; Githumbi et al., 2022a). This model estimates the relative abundance of plant taxa, along with the standard error of these estimates, given pollen counts and input parameters that represent sedimentary basin size and type, pollen productivity estimates (PPEs), pollen fall speeds, and atmospheric conditions. REVEALS was developed to operate at the regional scale (Hellman et al., 2008a, b; Sugita, 2007a); inferences of plant relative abundance represent the background vegetation over large areas (suggested as 100 km × 100 km by Hellman et al. (2008b), but this scale is variable). REVEALS has traditionally been used to infer plant relative abundance from records from large lakes (> 50 ha) but has been tested and applied to regions with records from a number of smaller lakes. The REVEALS model accounts for both differential productivity and dispersal among taxa. Differential productivity is determined by taxon-specific PPEs, while dispersal is modeled according to a Gaussian plume (Sutton, 1953) or Lagrangian dispersal–deposition model (Kuparinen et al., 2007), both of which require the specification of atmospheric conditions including wind speed. REVEALS accounts for differential dispersibility among taxa using pollen fall speeds; see Githumbi et al. (2022a) and Sugita (2007a) for a more detailed and theoretical description of REVEALS. We implement REVEALS using the REVEALSinR R package (Theuerkauf et al., 2016). REVEALS estimates for other regions included in the LandCover6k effort (Githumbi et al., 2022a; Li et al., 2023) were developed using more traditional implementations of this model (LRA.REVEALS.v6.2.4.exe (Sugita, unpublished) and the LRA R package (Abraham et al., 2014)), which differ slightly in their calculation of the standard errors of relative abundances.

Pollen source areas and the relative representation of plant taxa in the REVEALS dispersal–deposition model are affected by sedimentary basin type (e.g., lake, mire) and area (Sugita, 2007a; Trondman et al., 2016). Basin type is typically included in Neotoma metadata for pollen datasets, but not all datasets include metadata on basin area. To determine basin area for these datasets, we developed a standard workflow (Goring, 2024). Firstly, we used hydrological databases, National Hydrography Dataset (United States Geological Survey, 2022) and National Hydro Network (Natural Resources Canada, 2022), to assign basin areas to datasets whose coordinates fell within a waterbody polygon. Secondly, for dataset coordinates that landed outside a waterbody polygon, we used Google Earth Engine to identify the basin. These basins were traced using the polygon tool in Google Earth Engine, and basin area was calculated from polygon area. Not all basins could be identified, however, particularly for pre-GPS sites in Neotoma with imprecise coordinates. In total, we determined basin area for 545 of the 1445 records. For the remaining sites still without basin area, we assigned a size of 50 ha (900 of 1445 records). In the context of the REVEALS model, this represents a medium-sized lake. This decision avoids the potential biases from assigning large or small lake areas, although site-level reconstructions may over- or under-represent taxa if basin area (and hence pollen source area) is inaccurate (Jackson, 1990; Davis, 2000, p. 200; Liu et al., 2022). All basin areas recovered in the first and second steps were added as site-level metadata to Neotoma, along with dataset notes.

We used PPE and fall speed datasets from Wieczorek and Herzschuh (2020) for the Northern Hemisphere extra-tropics. Specifically, we used the North American continental-scale datasets, which include PPE (with grass as the reference taxon) and fall speed values for 30 of the 32 taxa we consider in this work. For *Ambrosia* (ragweed) and *Tsuga* (hemlock), which were not included in Wieczorek and Herzschuh (2020), we use PPE and fall speed values from a previously compiled North American dataset (Dawson et al., 2016; Trachsel et al., 2020). Additionally, for the *Larix* (larch) fall speed, we used the value for *Larix laricina* from Niklas (1984), which is the dominant species in eastern and northern North America. This estimate is 1 order of magnitude smaller than the *Larix* taxon-level fall speed estimate included in Wieczorek and Herzschuh (2020), which originates from Bodmer (1922). We experimented with fall speed datasets that included these larger *Larix* fall speed estimates; these vegetation reconstructions appeared to over-represent *Larix*. These challenges associated with dealing with the heavy *Larix* pollen are described in Sjögren et al. (2008).

We used the Gaussian plume dispersal model with a wind speed of $3\,\mathrm{m\,s^{-1}}$ and neutral atmospheric conditions (vertical diffusion coefficient $cz = 0.12$; turbulence parameter $n = 0.25$; wind speed $u = 3\,\mathrm{m\,s^{-1}}$; see Jackson and Lyford, 1999), to be consistent with the dispersal model specified in the LandCover6k protocol for Northern Hemisphere reconstructions (Dawson et al., 2018; Githumbi et al., 2022a). We set the region cutoff to the REVEALSinR function default of 100 km; this specifies the maximum distance that most pollen will originate from (Sugita, 2007a; Theuerkauf et al., 2016).

We reconstructed land cover for 25 time intervals that cover the Holocene. These time intervals were defined

according to the LandCover6k Working Group protocol (Trondman et al., 2015) (Table S4). Time intervals are specified in kiloyears before present (ka), where present is defined as 1950 CE, but, for time intervals < 1 ka, we also note the Common Era (CE) timescale. Intervals in the period from 11.7 to 0.7 ka have a 500-year temporal grain (11.7 to 11.2 ka, 11.2 to 10.7 ka, etc.), while the three most recent intervals have a finer temporal grain (0.7–0.35 ka, 1250–1600 CE, 350 years; 0.35–0.1 ka, 1600–1850 CE, 250 years; 0.1–(−0.074) ka, 1850–2024 CE, 174 years) in order to better capture the changes associated with intensifying anthropogenic land use over the last 5 centuries. Pollen samples were assigned to a time interval based on their mean calibrated radiocarbon age. If multiple samples for a record fell within the same interval, pollen counts were summed by taxon, so each record would have at most one set of pollen counts per time interval. We used a grid resolution of $1° \times 1°$ (ca. 100 km × 100 km), also as specified by the LandCover6k protocol in order to facilitate use for Earth system modeling. Within a grid cell, REVEALS reconstructions for multiple sites were averaged, as is standard practice (Sugita, 2007a). Taxon-level reconstructions were aggregated to three land cover categories (Table S2): summergreen trees and shrubs (STS); evergreen trees and shrubs (ETS); and open vegetation/land (OVL), which includes grasses, herbs, and low-stature shrubs. Note that bare ground cannot be detected by pollen-based land cover mapping, so it is not included as a potential land cover type; presumably this missing land cover type is usually misclassified as OVL. All trees and shrubs (ATS) is calculated as the sum of STS and ETS.

2.3 REVEALS-GMRF (spatial modeling and interpolation with uncertainty)

We use the REVEALS-GMRF Bayesian hierarchical model (Pirzamanbein et al., 2018) to spatially interpolate the REVEALS-based land cover reconstructions. REVEALS-GMRF exploits the spatial dependence in land cover using a Gaussian Markov random field and permits the characterization of uncertainty given the empirical land cover product. As in Pirzamanbein et al. (2018), we use elevation as a covariate. Although including simulations of land cover as an additional covariate can further improve the reliability of resulting land cover maps (Pirzamanbein et al., 2020), the intent of our work is to develop a spatial land cover product suitable for validation of and assimilation with models of dynamic vegetation, land use, and the Earth system. Hence, to maintain independence, we refrain from using simulated land cover as a covariate. To quantify overall uncertainty of a grid cell for a specified time period, we computed the area of confidence regions (CRs; Pirzamanbein et al., 2018). Smaller CR values indicate higher confidence, while larger CR values indicate more uncertainty. As in Pirzamanbein et al. (2018), a CR threshold is determined using the complete set of CR values. Accordingly, any grid cells with a CR greater than a threshold of 9 were omitted from spatial reconstructions (Githumbi et al., 2022a). The result of this spatial interpolation is a set of empirically based land cover maps for North America and the LandCover6k time intervals, with uncertainty.

2.4 Calculation of proportional changes and mapped anomalies

To summarize continental-scale land cover dynamics through time, we built time series of (1) land cover relative to ice-free area for the time interval being mapped (here called relative-to-time-t mean land cover) and (2) land cover relative to ice-free land area at 0.25 ka (here called relative-to-modern mean land cover). Firstly, we set a fixed domain size by including only grid cells for which there were reconstructions for all time periods; this removes confounding effects that may arise from a changing number of included grid cells. Then we used recently updated ice sheet maps (Dalton et al., 2020) to identify glaciated and unglaciated grid cells for each time period and then calculated the fraction of unglaciated land cover for each time period. We did the same for pro-glacial and other lakes (Dyke and Prest, 1987; Peltier, 1994). We recognize that shorelines have changed over the Holocene but ultimately determined that the effect of this at the considered spatial resolution would be minimal (PALSEA (PALeo SEA level working group), 2010). We then calculated the relative-to-time-t mean land cover of each land cover type for each time period as the mean across all unglaciated grid cells at that time period. This metric usefully summarizes the relative proportions of land cover types within ice-free regions for any given time period, but, because both the numerator and denominator change over time, this metric does not track the overall increases in vegetated land area in North America during the last deglaciation. To calculate relative-to-modern mean land cover, for each time period, we multiplied the relative cover of each grid cell by the cell area and then summed the relative cover of each land cover type across space for unglaciated land grid cells. We then divide this summed relative cover by the sum of total unglaciated land area at 0.05 ka. Because this second metric uses a constant denominator that represents late Holocene deglaciated land area, the relative-to-modern metric of relative cover captures both the deglacial increase in available land in North America and changes in land cover proportion within that available land.

For each pair of time intervals, we calculated land cover change as grid-cell-scale differences for each of the three land cover classes. After visually identifying areas of large land cover changes (Fig. S3 in the Supplement), we hand-selected several regions for further investigation, choosing areas with large changes and/or few prior regional reviews: the northeastern US and southeastern Canada (NEUS/SEC); eastern Canada (ECAN); western Canada and Alaska (WCAN/AK); and the Pacific Coast, Cascades, and

Sierra Nevada (PCCS). We then assessed vegetation change for each region at both the taxon and land cover scales, using the REVEALS grid-cell estimates of taxon mean abundances and the REVEALS-GMRF interpolated estimates of mean cover for the land cover types.

3 Results

3.1 Data coverage

The assembled dataset of 1445 fossil pollen records has good coverage across the continental US and Canada (Figs. 1a, S1). Areas of relatively high site density include the Great Lakes region of the US and Canada, the northeastern US, the Rocky Mountains, the Pacific Coast, and central Alaska. Given good data mobilization efforts for the US and Canada, this distribution reasonably approximates the true distribution of fossil pollen records, so spatial gaps usually represent a lack of available sites (e.g., few lakes or wetlands in arid regions) or inaccessibility (e.g., high Arctic). Conversely, a lower site density in Mexico and Central America is partially due to less extensive open-data mobilization efforts in these regions. Temporally, the distribution of oldest samples (an indicator of record length) is smooth (Fig. 1b), with rapid accumulation of sites between 11.7 and 11 ka (33 % of sites have an oldest sample in this interval) and between 0.5 and −0.074 ka (74 % of sites have a youngest sample in this interval).

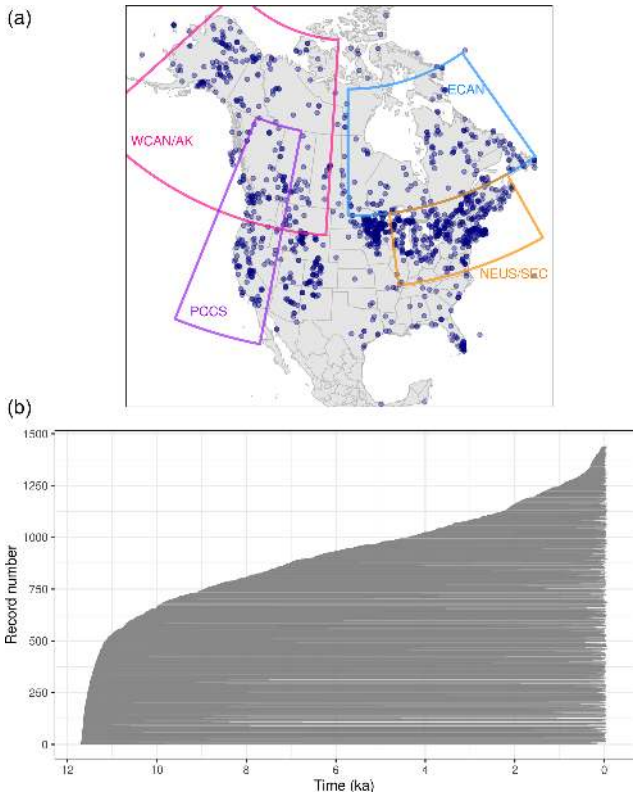


Figure 1. Spatiotemporal distribution of fossil pollen data used here. **(a)** Map indicating the distribution of sites recovered from the Neotoma Paleoecology Database and the case study regions (WCAN/AK: western Canada and Alaska; PCCS: Pacific Coast, Cascades, and Sierra Nevada; ECAN: eastern Canada; and NEUS/SEC: northeastern US and southeastern Canada). **(b)** Temporal extent of all sites, in which each site is represented by a horizontal gray line between the site's oldest and youngest Holocene samples. Sites are ordered by age of the oldest sample, reported as ka. Samples older than 11.7 ka are not shown.

3.2 Continental-scale trends in Holocene land cover

At a continental scale, the spatial configuration of land cover in North America has been broadly stable during the Holocene (Fig. 2). Persistent features include belts of high evergreen tree cover in the mountainous west and Canada; high summergreen tree cover in the eastern US; moderate to high cover of summergreen trees and shrubs in Alaska and northern Canada; and high proportions of open vegetation in the Great Plains, western Alaska, and Arctic Canada (Fig. 2).

However, despite this broadly stable spatial configuration, there were large continental-scale changes in the relative-to-modern fractional land cover types in North America during the Holocene, particularly during the early Holocene (Figs. 3a, S5). From 11.7 to 7 ka, the relative-to-modern fraction of forested land cover increased from about 42 % to 61 %. This increase closely tracked the increase in available land surface area, as the Laurentide Ice Sheet retreated (Fig. 3a) (Dalton et al., 2020). During the early Holocene, the largest gains in forest cover were across deglaciated western Canada and ice-marginal areas in eastern Canada (Figs. 2, S5). Forest cover continued to expand between 7.5 and 4.5 ka (Fig. 3a), even though the Laurentide Ice Sheet had disappeared by ∼ 6 ka, with the largest afforestation in the northern Great Plains of central Canada and in recently deglaciated regions of eastern Canada (Figs. 2, S5). Continental-scale forest cover remained stable from 4.5 to 1.5 ka then declined after 1.5 ka (Fig. 3a). The late Holocene decline in forest cover was most pronounced in the eastern US and in Arctic and boreal Canada, where open vegetation began increasing after 4 ka (Figs. 2, S5, S6).

Within these Holocene trends, the three land cover types followed differing trajectories (Fig. 3b). All three show a strong increase between 11.7 and 7.5 ka in their relative-to-modern land cover, again tracking ice retreat. After 7.5 ka, however, the three trajectories diverged. Evergreen trees and shrubs continued to rise slowly but steadily from 7.5 to 2 ka then declined slightly (Fig. 3b). Summergreen trees and shrubs reached peak extent at 4.5 ka then declined, with an accelerated decline after 1.5 ka. The proportion of open lands remained largely stable from 7.5 to 4.5 ka then increased, with an accelerating increase after 2 ka. A close examination of the continental-scale anomaly maps (Figs. S5, S6) indicates a fairly complex spatial mosaic for each land cover

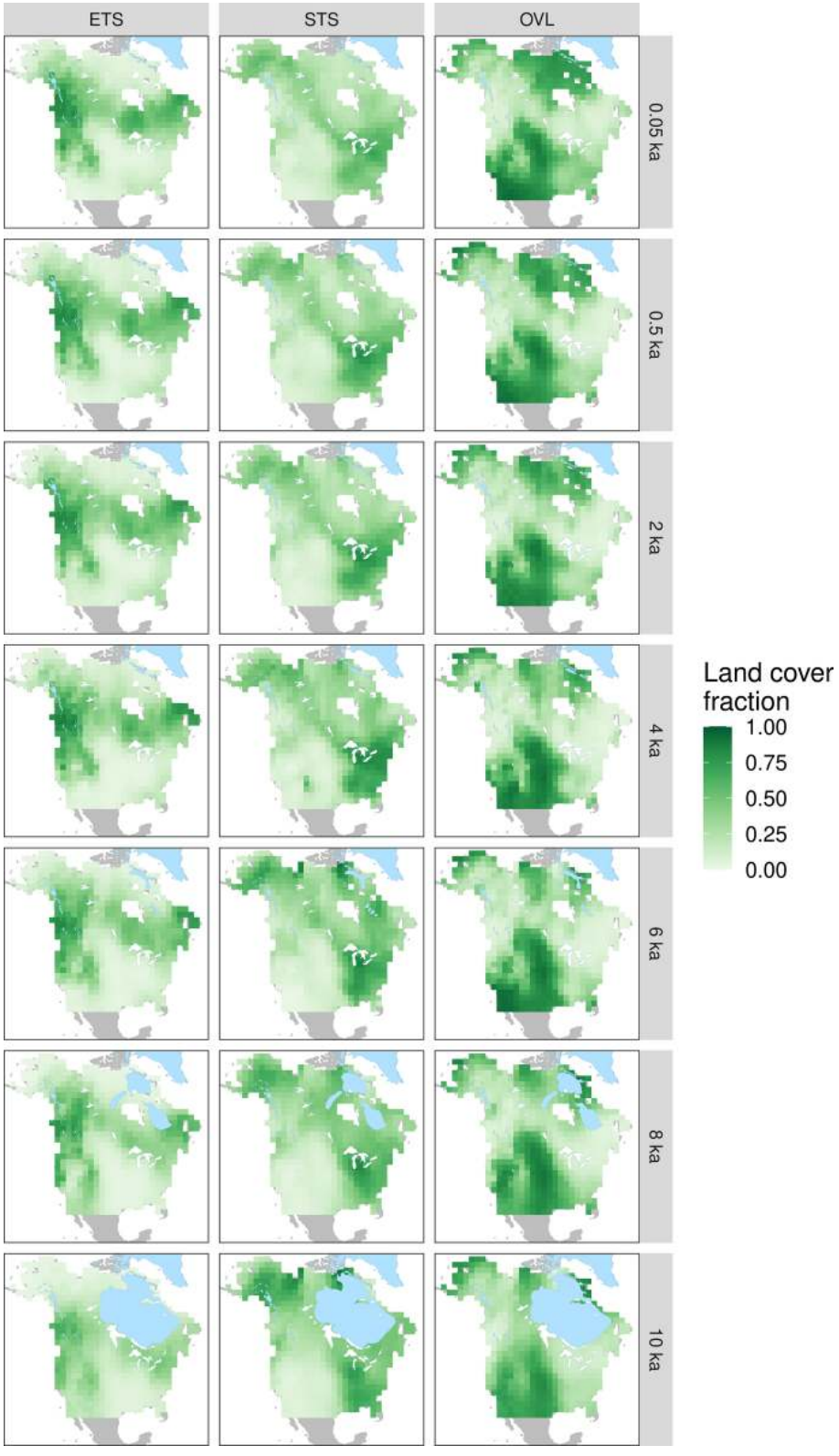


Figure 2. Interpolated REVEALS-based estimates of fractional cover for evergreen trees and shrubs (ETS), summergreen trees and shrubs (STS), and open vegetation/land (OVL). Laurentide and Cordilleran ice sheet extents (Dalton et al., 2020) are indicated by gray polygons. Estimates are presented on a $1° \times 1°$ grid, for selected time periods, with ages reported as ka. Map ordering follows the geological convention of oldest maps at the bottom. The spatial domain for interpolation includes all unglaciated locations in North America between 17 and 79° N.

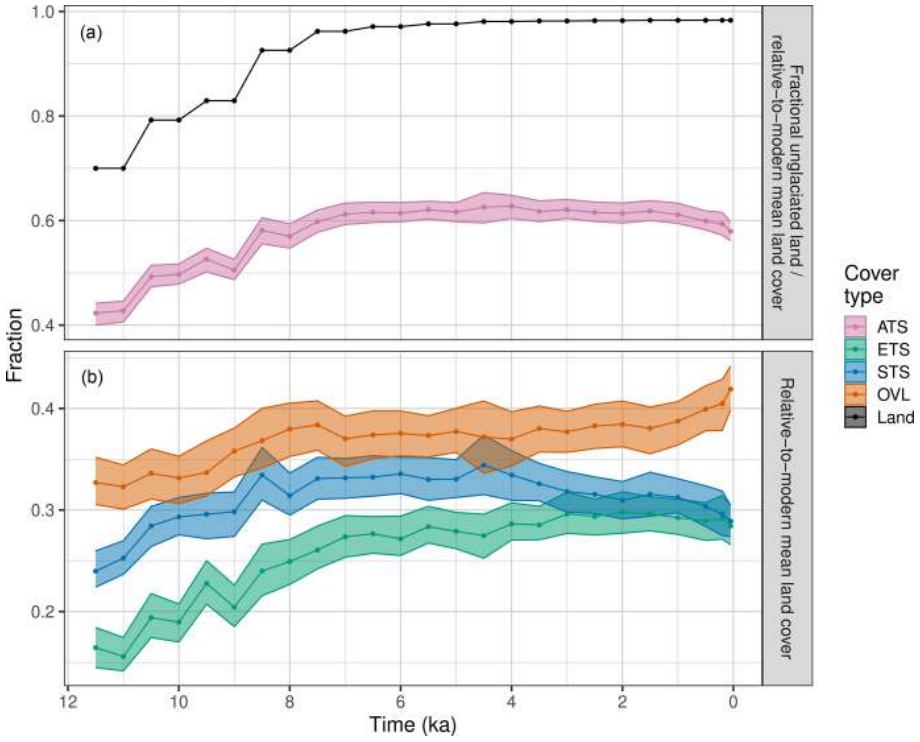


Figure 3. **(a)** Holocene trends in relative-to-modern mean land cover for all trees and shrubs (ATS) in North America (pink curve with 95 % uncertainty envelope), expressed relative to present unglaciated land area (see Data and methods), and the fraction of unglaciated land relative to continental land area (black). ATS is the sum of evergreen and summergreen trees and shrubs. **(b)** Trends in the relative-to-modern mean land cover of evergreen (ETS), summergreen (STS), and open vegetation/land (OVL) for North America. For both plots, land cover estimates are based on interpolated data for the spatial domain shown in Fig. 2.

type, with the continental-scale trends emerging from a welter of regional-scale phenomena. For example, widespread gains in evergreen trees and shrubs across much of Canada and Alaska between 6 and 4 ka were partially offset by large losses in the eastern US and southeastern Canada over the same period (Fig. S5). Because different plant species predominate in different regions of North America, these continental-scale trends in land cover were the emergent outcomes of individualistic species-level responses to changing climates and, in some places, intensifying land use (Williams et al., 2004).

3.3 Regional case studies

3.3.1 Northeastern US and southeastern Canada (NEUS/SEC)

For the mostly forested NEUS/SEC, after initial afforestation and loss of open lands during the early Holocene (10 to 8 ka), the principal dynamic has been shifts in the relative cover of evergreen and summergreen trees and shrubs (Figs. 4a, S7). The relative-to-time-t fractional cover of evergreen trees and shrubs declined throughout the early to middle Holocene (10 to 4 ka) in the southern part of the domain, which intensified to widespread loss across the NEUS/SEC (6 to 4 ka), but then reversed after 4 ka, with recovery and regrowth of evergreen trees and shrubs (Fig. 4a). The western increase in open lands between 8 and 4 ka is caused by the eastward expansion of prairie due to drier conditions (Williams et al., 2009b), while the decrease in open lands from 4 to 0.5 ka is due to increased moisture availability that resulted in a westward shift in the prairie–forest border and an increase in summergreen forest taxa in the eastern Midwest (Umbanhowar et al., 2006). Overall, the low proportions of open vegetation in the NEUS/SEC from 9 ka until European settlement (Fig. 4b) likely represent these western prairies and local wetlands, which expanded in the late Holocene in parts of the NEUS/SEC (Brugam and Swain, 2000; Ireland and Booth, 2010), rather than grasslands or other open lands in eastern deciduous forests (Faison et al., 2006).

At a taxon level, most changes in evergreen cover can be attributed to regional declines in cold-tolerant conifers such as *Picea glauca*, *P. mariana*, and *P. rubens* (white, black, and red spruce); *Pinus banksiana*, *P. resinosa*, and *P. strobus* (jack, red, and white pine); and *Abies balsamea* (balsam fir) between 10 and 6 ka (Figs. 4c, S8) (Spear et al., 1994; Jackson and Whitehead, 1991; Jackson et al., 1997). These changes, combined with the zonal pattern of evergreen expansion in the northern NEUS/SEC and declines in the south-

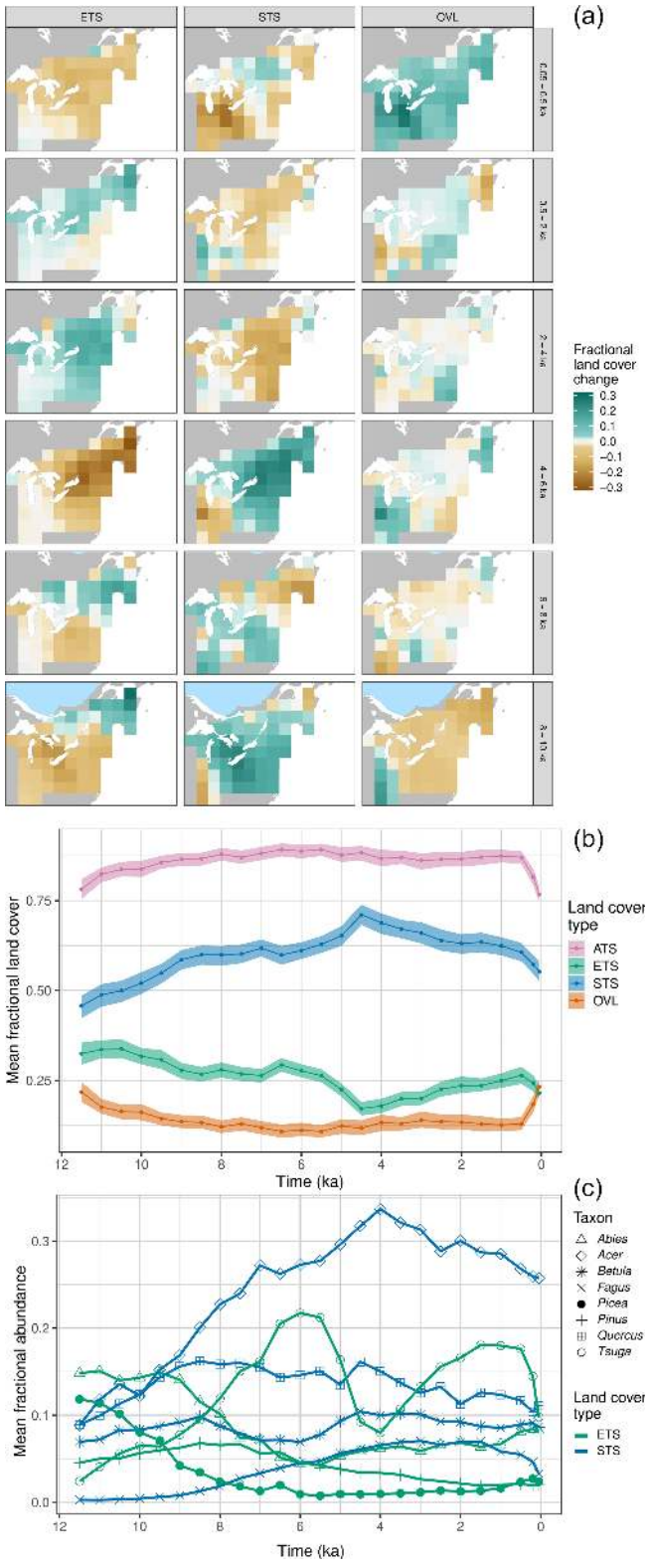


Figure 4. **(a)** Land cover anomaly maps for the northeastern US and southeastern Canada (NEUS/SEC) case study region. Maps show the anomalies in fractional cover for each land cover class for pairs of indicated time intervals. Spatial resolution is $1° \times 1°$, and time units are ka. **(b)** Holocene trends in the relative-to-time-t mean fractional cover of the three land cover types (ETS, STS, OVL) and the ATS sum for the uninterpolated REVEALS grid cell estimates across the NEUS/SEC region. **(c)** Holocene trends for the REVEALS relative-to-time-t abundance estimates for the six most commonly occurring taxa in the region. Line color indicates assignment of individual taxa to land cover types. For taxon-level maps, see Fig. S8.

ern part, suggest that much of the evergreen tree and shrub cover changes during the early to middle Holocene can be attributed to postglacial northward shifts in tree distributions in response to rising temperatures and deglaciation.

A second major feature is the well-known and dramatic expansion, collapse, and re-expansion of *Tsuga canadensis* (eastern hemlock), a cool-temperate conifer that typically occupies warmer climates than *Abies balsamea* (Thompson et al., 1999). Investigations continue into understanding the abrupt and widespread collapse in *Tsuga canadensis*, which differed from the overall evergreen trend. The collapse occurred in less than 10 years at some sites (Allison et al., 1986) and is linked to regional shifts in water availability and temperature gradients (Booth et al., 2012; Foster et al., 2006; Haas and McAndrews, 1999; Shuman et al., 2023). Initial hypotheses that a pest or pathogen such as *Lambdina fiscellaria* (hemlock looper) (Bhiry and Filion, 1996; Davis, 1981; Anderson et al., 1986) caused the *Tsuga* decline have not been supported by recent investigations (Oswald et al., 2017), although insect remains are scarce in lacustrine archives. Understanding the causes of the hemlock collapse is outside the scope of this paper; however, this paper shows its importance in that a single-species collapse fundamentally altered the functional composition, ecosystem phenology, and land cover of the NEUS/SEC for thousands of years.

Among summergreen taxa, these REVEALS reconstructions indicate a strong growth in *Acer* (maple) cover in the NEUS/SEC until 4 ka and a decline thereafter. *Acer saccharum* (sugar maple) is probably the dominant taxon driving this curve, with *A. rubrum* (red maple) increasing in the late Holocene (Finkelstein et al., 2006). *Quercus* (oak) abundances were high between 9 and 4.5 ka, then steadily declined, while *Betula* (birch) abundances remained relatively stable. *Fagus grandifolia* (American beech) abundances continued to steadily increase throughout this period until 3 ka then began declining after 1.5 ka, along with *Tsuga canadensis*, while *Abies balsamea* abundances increased. Disturbance-related taxa and indicators of open vegetation such as *Ambrosia* and *Rumex* (sorrel; not shown) begin increasing at ca. 0.35 ka (1600 CE). These late Holocene changes in forest composition can plausibly be attributed to regional cooling (explaining the increase in *Abies balsamea*) and perhaps also intensified human land use and disturbance, with the relative importance of these drivers varying at subregional scales and among taxa (Oswald et al., 2020; Mottl et al., 2021).

An intriguing feature of these REVEALS reconstructions is the inference of *Abies balsamea* and *Acer* as the most common evergreen and summergreen tree taxa in the NEUS/SEC, given that *Picea*, *Pinus*, and *Quercus* are more abundant in pollen and macrofossil records and that prior site-level and regional syntheses of Holocene pollen records have emphasized their dynamics (Jackson et al., 1997; Jackson and Whitehead, 1991; Payette et al., 2022; Spear et al., 1994). Witness tree data in the NEUS also indicate that *Fagus* and *Quercus* were the most abundant broadleaved taxa at the time of European settlement (Thompson et al., 2013). One possible reason for the higher levels of *Abies* and *Acer* reported here is that our NEUS/SEC domain extends a bit farther north than prior reconstructions that have focused more on central and southern New England. A second possibility is that the parameterizations for *Abies* and *Acer* are incorrect, causing the coverages of these taxa to be overestimated (see Discussion).

3.3.2 Eastern Canada (ECAN)

In eastern Canada (ECAN), immediately north of the NEUS/SEC, the relative-to-time-*t* fraction of evergreen trees and shrubs increased across the entire region until 4 ka, with slower and more spatially heterogeneous expansion of evergreen cover between 4 and 2 ka (Figs. 5a, S9). After 4 ka, open vegetation expanded (Fig. 5a, b). This expansion of evergreen trees and shrubs can be traced to separate phases of expansion for *Abies balsamea* and *Picea*, with *A. balsamea* expansion mostly between 11.5 and 7.5 ka (in the southern portion) and *Picea* expansion mostly between 7.5 and 3 ka, across the area and especially in the central portion (Figs. 5c, S10). Increasing Cyperaceae abundance after 3.5 ka signals the expansion of forest–tundra. Major hardwood summergreen taxa include *Betula* and *Alnus*. *Alnus* abundances expanded until 6 ka then slowly declined, while *Betula* abundances expanded between 8.5 and 6 ka then also declined. These declines in *Alnus* and *Betula* after 6 ka co-occurred with expansions of *Picea* and Cyperaceae, suggesting that the regional vegetation shifted from more of a mixed forest or woodland in the early Holocene to evergreen coniferous forest, forest–tundra, or tundra in the middle to late Holocene. Note that *Populus* is not included in these REVEALS reconstructions, but it is an important taxon in ECAN (Peros et al., 2008), and its omission may cause an underestimate of summergreen cover.

These vegetation changes in ECAN can be attributed to a combination of deglaciation, changing temperatures, and fire history. The Laurentide Ice Sheet collapsed at 8.4 ka, and the last remnants of the Labrador Dome disappeared from northern Quebec by 5.7 ka (Dalton et al., 2020). The replacement of open land by forest cover during the early Holocene was driven primarily by increases in evergreen trees and shrubs. The open forests at this time lack modern analogues and varied spatially in taxonomic composition, with more *Abies* and *Betula* to the east and *Picea* toward the west (Richard et al., 2020). By 7.5 ka, closed forests developed in response to warmer temperatures. This was followed by a decrease in summergreen taxa in the southern portion of the boreal forest and a decline in *Abies* in the lichen woodland and feather moss forest toward the west (Fréchette et al., 2021; Richard et al., 2020). In the lichen woodlands of the north, shrub *Betula* and *Betula papyrifera* (paper birch) decreased after 6 ka, although they remained high in the southwest (Fréchette et

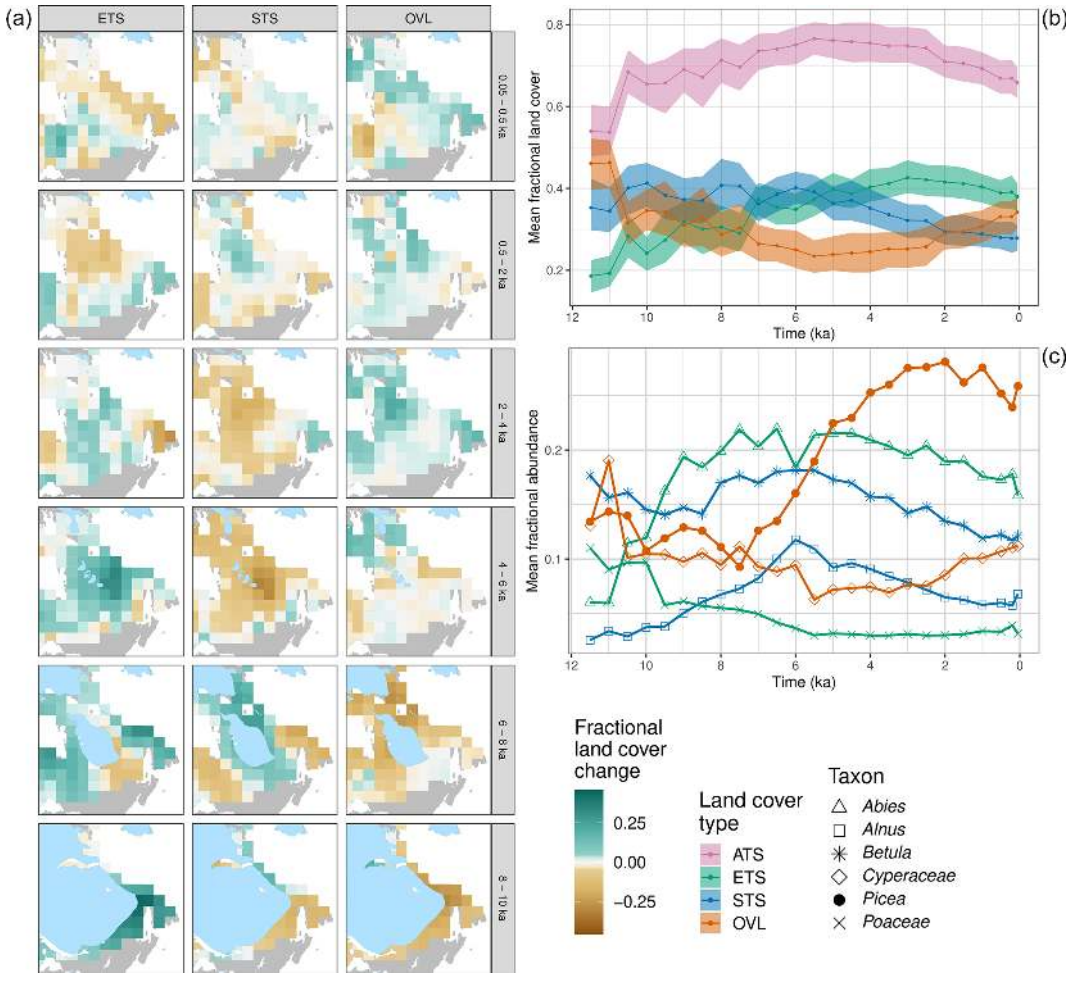


Figure 5. **(a)** Land cover difference maps for ETS, STS, and OVL for the eastern Canada (ECAN) case study. **(b)** Holocene trends in the relative-to-time-*t* mean land cover of the three land cover types (ETS, STS, OVL) and the ATS sum for the uninterpolated REVEALS grid cell estimates across the ECAN region. **(c)** Holocene trends for the REVEALS abundance estimates for the six most commonly occurring taxa in the region. For both panels, figure conventions follow Fig. 4. For taxon-level maps, see Fig. S10.

al., 2018). Near the treeline, *Picea* forests were more open between 7 and 4 ka, with *Alnus* and shrub *Betula* more abundant (Fréchette et al., 2018; Gajewski, 2019). In ECAN, *Picea* abundances reached a maximum between 4 and 2 ka (Fréchette et al., 2018), with the southern portion of the forest tundra becoming lichen woodland at this time. After 2 ka, *Picea* abundances at northern sites declined and open lands increased in response to cooling, but the timing and rate of *Picea* losses varied among sites and are governed in part by fire history (Gajewski et al., 2021; Gajewski, 2019).

3.3.3 Western Canada and Alaska (WCAN/AK)

In western Canada and Alaska (WCAN/AK), the relative-to-time-*t* mean land cover for evergreen trees and shrubs rapidly expanded between 11 and 8 ka, while the coverage of summergreen trees and shrubs and open lands decreased (Figs. 6a, b, S11). Most of Alaska was not glaciated during the Last Glacial Maximum; however, much of western Canada, the Brooks Range in Alaska, and southern coastal Alaska were covered by ice (Dalton et al., 2020). Evergreen tree species such as *Picea glauca* (white spruce) persisted in this region in local microrefugia (Anderson et al., 2006) then expanded their ranges during end-Pleistocene warming and deglaciation. Other evergreen taxa such as *Pinus contorta* (lodgepole pine) expanded northward with deglaciation (MacDonald and Cwynar, 1991). Trends in taxon abundances differ substantially between the western and eastern subregions (Figs. 6c, S12). In the eastern subregion, changes in taxon abundances were muted, with a modest expansion in *Picea* and *Tsuga* between 11.5 and 7.5 ka and a slow decline in *Betula* between 10 and 6 ka. *Tsuga* (mostly *Tsuga heterophylla*; western hemlock), which occurs primarily along the coast, was abundant along the southern coastal areas by 11 ka (Lacourse et al., 2012; Lacourse and Adeleye, 2022), arrived by 9.5 ka in southeastern Alaska (Hansen and En-

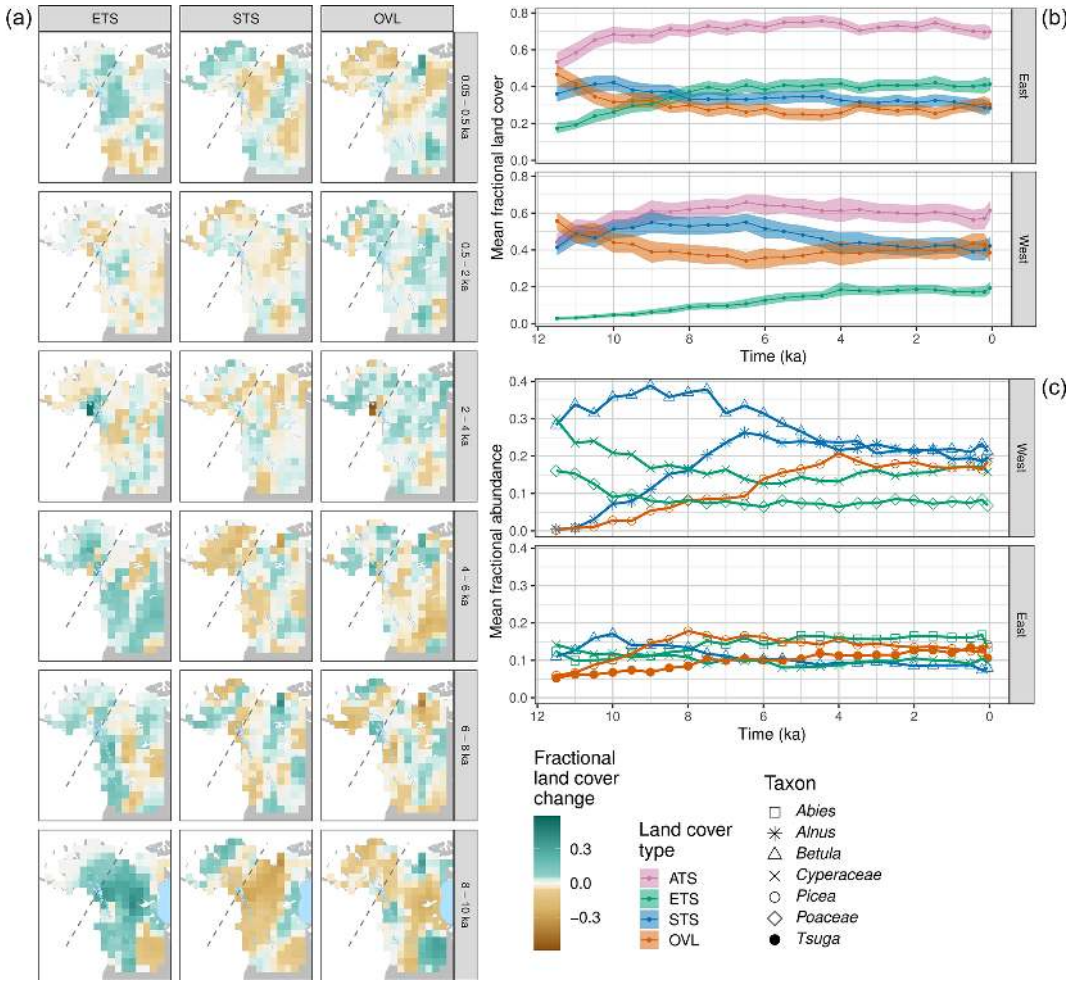


Figure 6. **(a)** Land cover difference maps for the western Canada/Alaska (WCAN/AK) case study region. **(b)** Holocene trends in the relative-to-time-*t* mean fractional cover of the three land cover types (ETS, STS, OVL) and the ATS sum for the uninterpolated REVEALS grid cell estimates across the WCAN/AK region, with grid cells averaged separately for eastern and western subregions (dividing line shown in panel **(a)** as a dashed line). **(c)** Holocene trends for the REVEALS abundance estimates for the six most commonly occurring taxa in the region, with grid cells averaged separately for eastern and western subregions. For both panels, figure conventions follow Fig. 4. For taxon-level maps, see Fig. S12.

gstrom, 1996; George et al., 2023), increased in abundance along the southern coastal areas by 8 ka, and then expanded during the mid- to late Holocene into southern central Alaska (Anderson et al., 2017) and the inland mesic forests of British Columbia (Rosenberg et al., 2003; Gavin et al., 2021). In the western part of this domain (mainly Alaska), changes in summergreen hardwood (mostly shrub) taxa predominate, with a major expansion of *Alnus* between 11.5 and 6.5 ka (Anderson and Brubaker, 1994; Cwynar and Spear, 1995) and a modest expansion of *Betula* between 11.5 and 9 ka. These expansions were accompanied by declines in Poaceae and Cyperaceae, with continued decline in Cyperaceae until 6 ka. *Picea* abundances steadily increased until 4 ka. The net effect was a decline in open vegetation and expansion of evergreen and summergreen trees and shrubs during the early to middle Holocene, with apparent region-wide stability after 4 ka (Anderson et al., 2019).

3.3.4 Pacific Coast, Cascades, and Sierra Nevada (PCCS) ranges

In contrast to the other regions, evergreen trees have dominated much of the land cover in the PCCS region since 12 ka (Figs. 7a, b, S13). In the northern subregion (often referred to as the Pacific Northwest), the relative-to-time-*t* proportions of cover types were fairly constant until 9 ka, after which summergreen and open land declined until 6 ka (Fig. 7a, b). However, taxon-level changes were very dynamic. From 11.7 to 10.5 ka, the REVEALS-estimated abundance of *Pseudotsuga menziesii* (Douglas fir) more than doubled, reflecting its arrival, expansion, and northward migra-

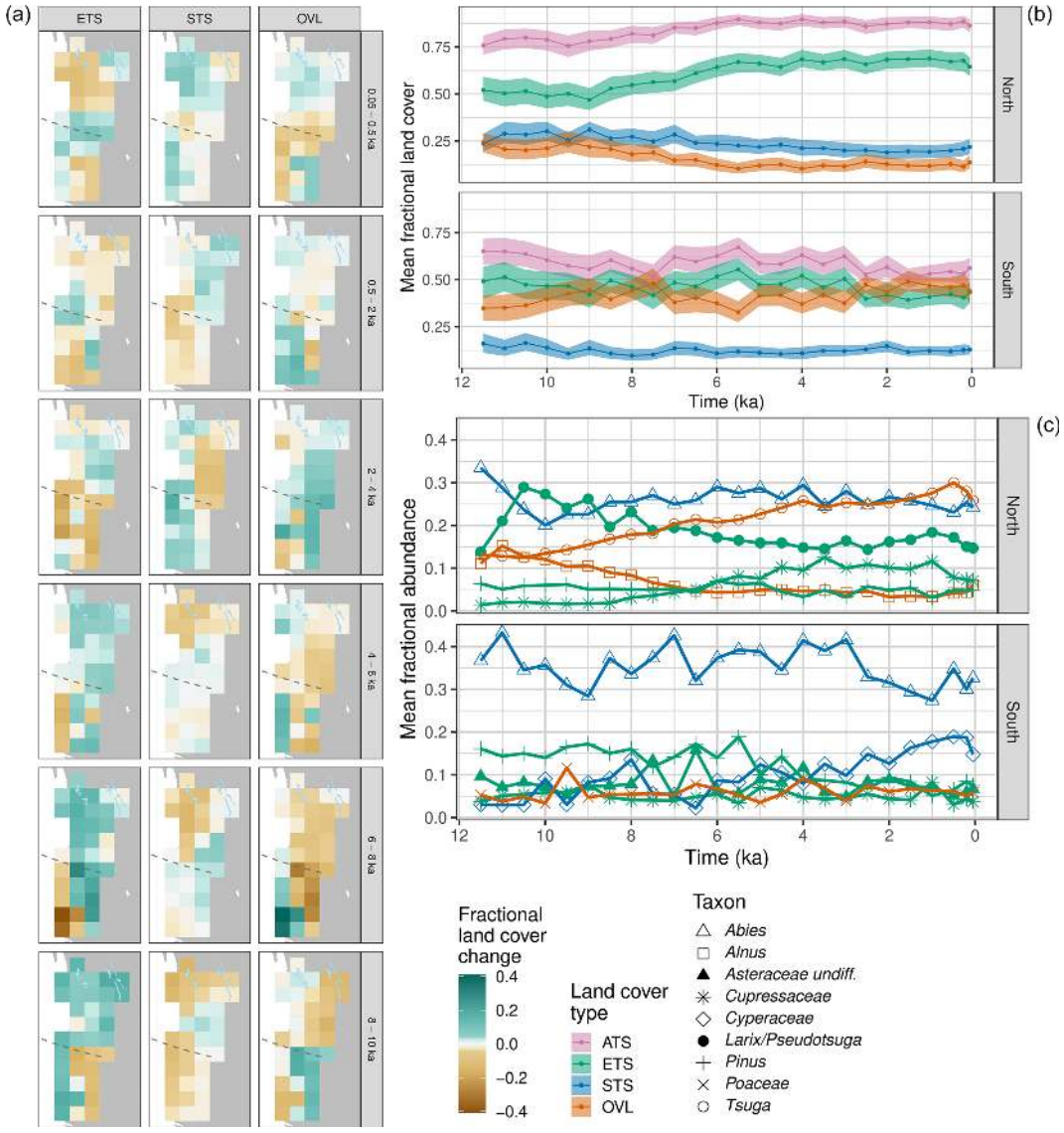


Figure 7. **(a)** Holocene trends in the mean relative cover of the three land cover types (ETS, STS, OVL) and the ATS sum for the uninterpolated REVEALS grid cell estimates across the Pacific Coast, Cascades, and Sierra Nevada (PCCS) case study region, with grid cells averaged separately for northern and southern subregions (dividing line shown in panel **(c)** as a vertical dashed line). **(b)** Holocene trends for the REVEALS abundance estimates for the nine most commonly occurring taxa in the region, with grid cells averaged separately for northern and southern subregions. For both panels, figure conventions follow Fig. 4. For taxon-level maps, see Fig. S14. **(c)** Land cover difference maps for the PCCS region.

tion (Gugger and Sugita, 2010) and replacing true firs (*Abies*) and *Picea* (Figs. 7c, S14). In the coastal ranges, frequent forest fires in the early Holocene contributed to a *Pseudotsuga–Alnus rubra* (red alder) association in the mountains (Gavin et al., 2013; Long et al., 1998, 2007) and a *Quercus* savanna (not shown) that was common in the lowlands (Walsh et al., 2008, 2010; Giuliano and Lacourse, 2023). Summergreen taxa (mostly *Alnus rubra*) and open land pollen indicators declined from 8 to 6 ka (Fig. 7b) and were replaced by shade-tolerant *Abies*, *Tsuga*, and Cupressaceae, which are mostly western red cedar in this region (Fig. 7b) (Lacourse, 2009; Gavin et al., 2013; Worona and Whitlock, 1995). After 6 ka, the overall abundance of conifer taxa remained constant (Fig. 7a, b), although the proportion of *Tsuga* and Cupressaceae increased steadily through the late Holocene while *Pseudotsuga* declined, consistent with less fire and the persistence of old-growth forest (Whitlock, 1992; Lacourse and Adeleye, 2022). Logging of the last century is associated with an increase in summergreen trees and shrubs and open land in the coastal regions (Fig. 7a) (Davis, 1973; Whitlock et al., 2018).

The most common taxon in these REVEALS reconstructions, *Abies*, varied little over the last 9 ka, but this genus represents several shade-tolerant species that collectively are common throughout the region: *A. lasiocarpa* (subalpine fir), *A. grandis* (grand fir), *A. amabilis* (Pacific silver fir), and *A. procera* (noble fir). As noted for the NEUS/SEC, the reconstructed values of *Abies* are likely too high because the REVEALS estimate of fall speed may be overestimated. *Pinus* also represents several species and was most abundant in the dry eastern areas where it was consistently abundant during the Holocene (Minckley et al., 2007). *Pseudotsuga* and *Larix* have indistinguishable pollen morphologies and are therefore grouped in the reconstructions; however, *Larix* is limited to the eastern edge of this region.

The southern subregion (the Sierra Nevada, the Klamath Mountains, the California Coast Ranges, and the interior Great Basin) supported roughly equal amounts of conifer forest and open land that overall had minor relative changes over the Holocene (Fig. 7a). Summergreen trees and shrubs have been infrequent contributors to land cover in this subregion. At the taxon level, *Abies* is again the most common component of reconstructed evergreen land cover across the region, although its abundance may be overrepresented in this parameterization of REVEALS (Fig. 7b). *Pinus* and *Quercus* were most abundant in the early Holocene, forming open forests and woodlands, especially in the Klamath Mountains and Sierra Nevada (Anderson, 1996; Briles et al., 2008) fire-prone forests east of the Cascade Range (Walsh et al., 2015). Most of the eastern portion of this subregion is the Great Basin shrub steppe, where the few pollen records that exist are from high-elevation sites and low-elevation wetlands that are sensitive to fluctuating water tables, recorded as large fluctuations in Cyperaceae pollen. Increases in open land cover taxa (*Cyperaceae*, *Poaceae*, *Asteraceae*) between 10–7.5 ka and after 3 ka in this region may reflect either local expansion of alpine meadows and wetlands or expansion of steppe more broadly (Mensing et al., 2008; Brugger and Rhode, 2020; Minckley et al., 2007; Thompson, 1992). However, desert, steppe, and other open land arid ecosystems are likely to be under-represented in these reconstructions, due to a scarcity of dryland sites. Furthermore, bare soil and rock cannot be detected using pollen-based land cover mapping, so this land cover type is missing in these reconstructions.

4 Discussion

4.1 Drivers of Holocene land cover change in North America: scaling from taxon-level regional dynamics to continental-scale trends

These continental-scale Holocene changes in land cover (Figs. 2–3) are an emergent outcome of the individualistic plant responses to deglaciation and multiple environmental changes, including seasonal temperatures, effective moisture, atmospheric carbon dioxide, sea level rise, soil development, fire and other disturbance regimes, and (at some locations during the late Holocene) human land use. As shown here (Figs. 4–7), this interplay differed spatially across North America, often with opposing trends (e.g., simultaneous increases in evergreen cover in some regions and decreases elsewhere) that partially offset at the continental scale.

The first-order continental-scale drivers of Holocene land cover change in North America were changing climates and the retreat and disappearance of the Laurentide Ice Sheet, particularly during the early Holocene (11.7 to 7.5 ka) and lasting until 5.7 ka, with the disappearance of remnant ice in the Labrador Dome in northern Quebec (Dalton et al., 2020). Deglaciation and an overall increase in land availability explains why all land cover types show an increase in relative-to-modern cover during the early Holocene, with evergreen taxa showing the greatest gain (Fig. 3). Continental temperatures also closely tracked the decline in ice area (Marsicek et al., 2018), and vegetation responded to both factors. Superimposed upon the early Holocene increase in relative-to-modern cover for all PFTs are gains and losses for each PFT at subregional scales (Figs. 4–7), which can be linked to climate-driven changes in plant abundances at local to landscape scales that scaled upwards to continental-scale shifts in plant distributions, with both within-range shifts in dominance and leading-edge and trailing-edge range dynamics for individual plant taxa (Payette et al., 2022; Williams et al., 2004; George et al., 2023; Dallmeyer et al., 2022; Anderson et al., 2017).

Leading-edge dynamics and range expansion of tree taxa appear to have been primarily controlled by the increasing availability of deglaciated land area, end-Pleistocene warming, the declining influence of ice sheets on regional climates and moisture availability (Alder and Hostetler, 2015; Bartlein et al., 2014), and ongoing expansion of plant taxa into areas of increased climate suitability (Payette et al., 2022; Williams et al., 2004; George et al., 2023; Dallmeyer et al., 2022). Declining ice extent favored moisture advection into eastern areas where most of the increase in summergreen tree taxa took place and reduced it in mid-continental North America, where most of the open vegetation increase developed (Shuman and Marsicek, 2016; Shuman et al., 2002; Liefert and Shuman, 2020). These changes in the patterns of moisture availability simultaneously favored the large increase from 10 to 6 ka in summergreen trees and shrubs in eastern North America south of the former Laurentide Ice Sheet and the increase in open land in the mid-continent (Figs. 5–6).

Declines in abundance and trailing-edge dynamics of tree taxa were likely governed by a combination of declining climate suitability and, in some places, fire regimes, in which many local populations failed to re-establish after one or more fire events. For example, in the high northern latitudes of Quebec and Labrador, the expansion of open lands over the last 3000 years (Fig. 5) can be attributed firstly to declining summer insolation and temperatures, caused by precessional changes in the Earth's orbit (Payette, 2021), but,

at local to landscape and centennial scales, loss of forest cover was asynchronous and caused by individual fire events (Payette et al., 2008; Gajewski et al., 2021). Similarly, in the southern Great Lakes region and NEUS, the late Pleistocene to early Holocene transition from conifer-dominated forests and parklands to summergreen forests (Fig. 4) was driven by rising temperatures and changes in effective moisture (Shuman et al., 2002, 2019) but accelerated locally by intensified fire regimes, with the timing and rate of conversion varying among sites (Jensen et al., 2021; Clark et al., 1996). The expansion and then retreat of the Great Plains prairies (Fig. 4) was driven by early Holocene aridification and middle to late Holocene increases in moisture availability, while fire may have facilitated prairie expansion but delayed its retreat (Williams et al., 2009b; Nelson et al., 2006; Umbanhowar et al., 2006). Throughout North America, forests and fire dynamically co-existed and interacted during the Holocene (Iglesias and Whitlock, 2020; Kelly et al., 2013), so whether fire causes transformative shifts in ecosystem type depends on its synergistic interactions with directional changes in climate and other factors (Napier and Chipman, 2021). Regardless of the role of fire or other disturbances, regional shifts in temperature and moisture availability are usually the first-order predictors of Holocene changes in vegetation composition (Dean et al., 1984; MacDonald, 1989; Calder and Shuman, 2017; Shuman et al., 2004; Nelson et al., 2006).

The relative proportion of evergreen and summergreen cover types may have been affected by changes in the length and intensity of the growing season during the Holocene, which is regulated by precessional variations in insolation. In particular, the broad peak in summergreen tree cover between 8.5 and 3.5 ka (Fig. 3) is consistent with the hypothesis that summergreen tree and shrub abundances in North America are partially regulated by summer insolation and temperatures (Delcourt and Delcourt, 1994; Williams et al., 2001). Summer insolation reached higher peak intensity but has a shorter seasonal duration in the early Holocene than during the late Holocene (Huybers, 2006; Jackson et al., 2009), which may have favored plants with summer deciduous phenology that could more effectively exploit available energy during a briefer but more intense growing season (Delcourt and Delcourt, 1994; Williams and Jackson, 2007; Edwards et al., 2005). Indeed, pollen-reconstructed and CCSM3-simulated changes in growing-degree days also peaked during the mid-Holocene, when forest cover was greatest, and several millennia after peak summer temperatures, likely because of differential responses of maximum summer temperatures and total growing season warmth to orbital and other forcings (Marsicek et al., 2018). This may in turn suggest a seasonal-scale feedback loop between summer insolation, deciduous phenology, and total summer warmth (see Sect. 4.2).

During the late Holocene, the growth of Indigenous populations and intensification of human land use in the Americas had increasing effects upon land cover. Understanding the interactions among past climate change, fire regime, and land use is a highly active area of research. Rates of vegetation change worldwide began to increase between 4.6 and 2.9 ka (Mottl et al., 2021), consistent with growing intensification and extent of land use (Stephens et al., 2019). The 7 to 10 ppm decrease in global CO_2 between 1570 and 1620 CE has been attributed to land abandonment and reforestation due to mass mortality of Indigenous populations in the Americas, caused by the spread of multiple pathogens (Lewis and Maslin, 2015). The best evidence for dense human populations and extensive land clearance in the Americas comes from Central America and tropical South America (Islebe et al., 1996; McMichael, 2020).

In the land cover reconstructions presented here, the increase in prevalence of open lands after 0.5 ka in North America and some subregions (Figs. 3, 4, 7) is attributable to land use, but the role of land use for earlier time periods remains unclear. Land use prior to Euro-American settlement clearly altered land cover at some sites in North America, but land use effects are not easily detected at the regional to continental scales addressed here. In North America, the distribution of radiocarbon dates from archeological contexts suggests that population levels remained relatively low until $\sim$ 7 ka, with increases between 7 and 2 ka and then rapid increases after 2 ka (Peros et al., 2010). Indigenous cultures in North America clearly engaged in activities that, in some areas, modified the composition and structure of forested and unforested landscapes for millennia (Ellis, 2021; Delcourt et al., 1986; Leopold and Boyd, 1999; Munoz et al., 2014). In densely populated regions, such as lands of the Iroquois Confederacy and the Cherokee Nation, southern Ontario, Cahokia, and the American Bottom, land use altered vegetation structure and composition at local to landscape scales, through management of fire regimes (Roos et al., 2018; Anderson and Carpenter, 1991), land clearance for agricultural crops (McAndrews and Turton, 2007), and silviculture (e.g., favoring the spread of nut-bearing trees; Munoz et al., 2014; Black et al., 2006). In western North America, the effects of anthropogenic activity on vegetation and fire is an active area of research, with several paleoecological studies indicating changes consistent with human influences on forest composition (Walsh et al., 2015; Knight et al., 2022; Lacourse et al., 2007). Because the scale of human action was strongest at local to landscape scales and varied in intensity within and among regions, its detection often requires highly focused, local- to regional-scale studies (Oswald et al., 2020; Roos, 2020; Lacourse et al., 2007; Knight et al., 2022; Munoz and Gajewski, 2010). These studies clearly indicate a high intersite variance in the level and detectability of human impact. At the continental scale, Gajewski et al. (2019) did not find clear correlations between human population abundance and pollen abundance, including taxa of economic use or disturbance taxa, and concluded impacts occurred at local to regional scales. Thus, at the regional to continental scales considered here, it is an open question whether the rich re-

lationships and diverse activities engaged by communities within their homelands led to detectable changes in land cover types. We expect that pollen-based land cover reconstructions will continue to contribute to interdisciplinary approaches to address anthropogenic fire and land cover change during the Holocene (Snitker et al., 2022).

In contrast, after the Euro-American arrival and expansion from 1492 onwards, North American ecosystems were massively transformed (Stegner and Spanbauer, 2023) by multiple anthropogenic processes. These include widespread forest conversion to agricultural and pastoral lands, intensive forest harvesting, massive hydrological change through dam construction and wetland drainage, introduction of exotic species and pests, and greatly increased fire activity and fire suppression (Klein Goldewijk et al., 2011; Foster and Aber, 2004). These land cover changes can be detected as an increase in open land from 0.5 ka onwards (Figs. 3, 4, 7).

4.2 Biophysical and biogeochemical vegetation–atmosphere feedbacks to Holocene climates

4.2.1 Holocene vegetation–atmosphere feedbacks: prior work and need for data constraints

This paper and the other REVEALS-based reconstructions for the Northern Hemisphere (Githumbi et al., 2022a; Li et al., 2023) now lay the foundation for a next generation of Holocene vegetation–atmosphere research with well-constrained land surface data. Many studies have explored the potential impacts of vegetation–atmosphere feedbacks on Holocene climate dynamics at hemispheric to global scales, but these studies have generally not employed well-constrained land cover reconstructions. Treeline shifts have been identified as an important regulator of Holocene vegetation–atmosphere feedbacks in the high northern latitudes (Kutzbach et al., 1996). In mid-Holocene atmosphere–vegetation model simulations, strong snow masking resulted in warming 3 times higher than with weak snow masking (Otto et al., 2011). More recent work has highlighted the importance of the type and density of forest cover in determining the albedo feedback and magnitude of snow masking (Loranty et al., 2014; Alessandri et al., 2021). Hence, because snow masking and surface albedo are important regulators of surface–atmosphere feedbacks in climate models, they are also an important source of uncertainty in Holocene climate simulations because of the limited availability of well-constrained reconstructions of past changes in vegetation type, structure, and density. Vegetation structure and topographic complexity also jointly govern surface roughness, which affects lower atmosphere temperature, humidity, wind speed, and soil moisture (Bonan, 2015) and is the dominant land cover influence on micrometeorological processes (Chen and Dirmeyer, 2016). The effects of changing surface roughness on past climate variability remain largely unexplored. This new generation of land cover reconstructions provided by LandCover6k is intended to support future Earth system model experiments on past vegetation–atmosphere feedbacks, with first results now available for Europe (Strandberg et al., 2022).

The role of vegetation feedbacks on terrestrial carbon sequestration and Holocene climate variations also remains largely unexplored, despite ice-core evidence that Holocene CO_2 increased from 260 to 285 ppm over the period from 8 to 1 ka (ca. 53 GtC) and despite no clear understanding of the source(s) of that carbon. Initial work, using carbon isotopic evidence and carbon cycle models, indicated that changes in terrestrial biomass were responsible for about two-thirds of this increase (Indermühle et al., 1999). More recent Earth system model simulations indicate an ocean source through a process of elimination, given simulations that both the atmosphere and the terrestrial biosphere were gaining carbon between 8 and 2 ka (Brovkin et al., 2019). Prior data-based reconstructions of terrestrial carbon sequestration, mostly restricted to the northern middle and upper latitudes, indicate net carbon sequestration in these regions for most of the Holocene. Peatlands in the upper latitudes of the Northern Hemisphere appear to have been continuously sequestering carbon throughout the Holocene, with a total sequestration across the Holocene of 500 ± 100 GtC (Loisel et al., 2017; Yu, 2012). Prior reconstructions from pollen data and the LPJ dynamic vegetation model suggest a terrestrial sequestration of 13.9 GtC between 9 and 6 ka and a 3.5 GtC release after 6 ka for aboveground biomass in the Northern Hemisphere $> 45°$ N (Williams et al., 2011a). Regional reconstructions for eastern Canada indicate a peak in terrestrial biomass at 7 ka, with a ca. 8.5 GtC sequestration due to afforestation between 11 and 7 ka and a ca. 2 GtC release after 7 ka (Blarquez and Aleman, 2015), suggesting that postglacial boreal forest dynamics in this region were a primary contribution to Northern Hemisphere aboveground carbon sequestration. In the upper Midwest, aboveground biomass doubled between 8 and 0 ka, sequestering 1.8 GtC (Raiho et al., 2022). Given these various well-constrained Holocene sinks in the atmosphere and terrestrial biosphere, the key unknown is the corresponding sources, with potential options including changes in ocean alkalinity (Brovkin et al., 2019), subtropical wetland reductions with waning Northern Hemisphere monsoons (Guo et al., 2012), and intensifying land use (Ruddiman, 2003). Balancing the Holocene carbon cycle in the atmosphere–biosphere–ocean system is a major problem in Earth system science. This new generation of LandCover6k vegetation reconstructions, combined with Earth system models, is the best avenue forward to sharpen our understanding of the role played by surface–atmosphere feedbacks in Holocene climate dynamics, both biogeophysical and biogeochemical.

4.2.2 Assessing recent modeling studies of the Holocene temperature conundrum

The Holocene temperature conundrum has been a major focus of paleoclimatic research over the last decade (Kaufman and Broadman, 2023; Liu et al., 2014), and research has invoked vegetation–atmosphere feedbacks to resolve this conundrum (Thompson et al., 2022). The Holocene temperature conundrum involves a discrepancy between proxy-based reconstructions of global temperature changes, mostly based on marine records, which indicate a mid-Holocene maximum and mid- to late Holocene cooling (Marcott et al., 2013), while transient model simulations show small but steady warming throughout the Holocene (Liu et al., 2014). Many explanations for this discrepancy have since been proposed (Kaufman and Broadman, 2023). Recent prescribed-vegetation experiments in climate models produce an early Holocene warming to a Holocene Thermal Maximum, followed by cooling towards the pre-industrial Holocene (Thompson et al., 2022), consistent with paleoclimatic proxies. Conversely, experiments that include drivers such as dust, ice cover, orbital forcing, and greenhouse gases without accounting for Northern Hemisphere vegetation changes do not result in a mid-Holocene Thermal Maximum (Thompson et al., 2022).

Our reconstructions suggest, however, that, for North America, the prescribed vegetation maps used by Thompson et al. (2022) overstate the magnitude of Holocene vegetation change. These prescribed-vegetation experiments for 9 and 6 ka fully replace all C_3 grasses with boreal forest for all locations north of 50° N (Thompson et al., 2022, Fig. S9). This pattern is qualitatively consistent with the early Holocene afforestation reported here (Fig. 2) but is inconsistent with the demonstrated persistence of tundra throughout the early and middle Holocene, particularly in WCAN/AK (Figs. 2, 6) and the Canadian High Arctic (Fig. 2). Similarly, the prescribed full replacement of C3 grasslands with temperate deciduous forest for the 9 and 6 ka experiments (Thompson et al., 2022, Fig. S9) is inconsistent with clear palynological evidence for the establishment of the Great Plains grassland by the early Holocene and prairie expansion during the early to middle Holocene (Figs. 2, S5) (Williams et al., 2009a). Hence, the Thompson et al. (2022) simulations should be viewed as useful experiments that show the potential sensitivity of Holocene climates to large vegetation changes, but these experiments likely overestimate the contribution of vegetation feedbacks to resolving the Holocene temperature conundrum.

4.2.3 Understudied Holocene vegetation–atmosphere feedbacks in North America

Our reconstructions also highlight several major features of North American vegetation dynamics that may have underappreciated effects on Holocene vegetation–atmosphere feedbacks and climate dynamics at regional to continental scales. Firstly, the mid-Holocene decline and recovery of *Tsuga canadensis* in the northeastern United States is an example of how single-species dynamics can drive fundamental changes in vegetational structure. Although the patterns and drivers of the *T. canadensis* decline have been extensively studied (Oswald and Foster, 2012; Oswald et al., 2017; Booth et al., 2012; Foster et al., 2006), the effects of the *T. canadensis* decline on Holocene climates are unknown. As the dominant evergreen conifer of cool-temperate eastern North America, the decline in *T. canadensis* at ca. 5 ka is the primary driver of the loss of ETS between 6 and 4 ka, while the gradual recovery of *T. canadensis* after 5 ka drives the corresponding increase in ETS (Fig. 4). This shift in dominance between summergreen and evergreen trees and shrubs, in turn, regulates the overall albedo of the land surface and particularly its seasonal range. During times of foliage, summergreen forests can have more than twice the albedo of evergreen forests (Hollinger et al., 2010), and summergreen forests exhibit much greater seasonal variability, with maximum values in full foliage being 20 %–50 % larger than annual lows. Secondly, the peak in summergreen tree cover between ca. 8.5 and 4.5 ka (Fig. 2) may indicate a seasonal-scale positive feedback loop between summer insolation, summergreen phenology, and summer temperatures. Studies have suggested that the late Pleistocene to early Holocene peak in summer insolation favored summergreen phenology and carbon acquisition strategies over evergreen strategies (Delcourt and Delcourt, 1994; Williams and Jackson, 2007). Studies from the Pacific Northwest and Alaska also show a peak in *Alnus* and other summergreen tree and shrub taxa during the early Holocene (Fig. 7c), coincident with the summer insolation maximum and local maxima in temperature (Gavin et al., 2013; Edwards et al., 2005; Whitlock, 1992). This climate-driven response, in turn, may have increased the seasonal range of albedo and surface temperatures, thereby further favoring summergreen strategies. This summergreen feedback might have also contributed to some summer cooling, due to the higher summer albedo of summergreen trees (Hollinger et al., 2010). As an alternative hypothesis, Herzschuh (2020) suggested that the Eurasian distribution of evergreen spruce-dominated and deciduous larch-dominated evergreen forests was due to historical contingencies and alternate stable states. Although many studies have explored the effect of early to middle Holocene afforestation on vegetation feedbacks in the northern latitudes (Brovkin et al., 2009; Kutzbach et al., 1996), to our knowledge, no paper has yet focused specifically on the seasonal feedback effects associated with shifting proportions of summergreen and evergreen trees and shrubs.

4.3 Uncertainties and limitations in pollen–vegetation model reconstructions

Land cover reconstructions from pollen rely upon a variety of pollen–vegetation models (PVMs), some of which have well-understood limitations and uncertainties and some of which are newer and are still being studied. The REVEALS PVM used here is has been widely adopted (Li et al., 2020; Githumbi et al., 2022b; Serge et al., 2023; Azuara et al., 2019; Hoevers et al., 2022) because it represents some of the taxon-level processes governing pollen production, transport, and representation (Prentice, 1985; Sugita, 2007a). However, processes such as atmospheric transport are simplified (Jackson and Lyford, 1999), and key parameters such as pollen productivity estimates (PPEs) carry uncertainties (Wieczorek and Herzschuh, 2020; Broström et al., 2008; Hayashi et al., 2022) that translate to uncertainties in fractional-weighted land cover area. Most PPE estimates are generated from models fitted to spatial networks of vegetation surveys and surface pollen samples, and these PPE estimates depend strongly on models of pollen dispersal (Theuerkauf et al., 2012).

Such issues may explain some of the surprising aspects of the reconstructions presented here. For example, reconstructed *Acer* cover in the NEUS/SEC (Fig. 4c) is high compared to settlement-era estimates from witness trees and land surveys (Thompson et al., 2013; Paciorek et al., 2016). Similarly, reconstructed cover of *Abies* in both the NEUS/SEC and PCCS is higher than expected (Figs. 4c, 7c). *Abies* and *Acer* are notoriously under-represented in fossil pollen assemblages (Bradshaw and Webb, 1985), relative to independent surveys of tree abundance in the surrounding ecosystems, due to the low pollen productivity of maple trees relative to other taxa (Finkelstein et al., 2006; Liu et al., 2022) and high fall speeds of *Abies* (Jackson and Lyford, 1999). Hence, a key value of process-based PVMs, such as REVEALS, is the ability to correct for these known biases. However, REVEALS estimates are sensitive to parameter choices, and it is possible that the estimates of *Abies* and *Acer* are too high. There are few estimates of *Abies* fall speeds compared to other taxa, and the fall speeds used here from Wieczorek and Herzschuh (2020) are similar to the values for *Larix* that initial testing indicated led to *Larix* overrepresentation. *Larix* is also challenging to model accurately in pollen–vegetation models because its large pollen grains do not disperse far. Hence, local populations of larch can be difficult to differentiate in pollen records from those occurring across the broader source area. Moreover, the scarcity of *Larix* pollen grains means that the REVEALS reconstructions are highly sensitive to its parameterizations for *Larix*.

REVEALS is not spatial or temporal in nature, so there is no representation of spatiotemporal dependencies among site-level reconstructions (Figs. S2, S3). REVEALS estimates of fractional cover uncertainty are based on the total number of pollen grains counted in a sample and the error associated with the PPEs but do not include process uncertainty or uncertainty in other model inputs. The GMRF serves as a post hoc interpolator to generate spatially complete vegetation reconstructions for each time period, but this approach does not mechanistically represent the underlying processes that link pollen to vegetation. Neither REVEALS nor the GMRF includes soil, slope, aspect, or other edaphic controls on vegetation cover. The REVEALS-GMRF workflow as currently implemented does not account for pollen sample age uncertainty. While the Bchron age–depth modeling approach is a Bayesian approach that estimates posterior distributions of sample ages, propagating this through the REVEALS-GMRF workflow would require the addition of temporal dependence in the interpolation model. Initial experiments to add temporal dependence have been computationally prohibitive; alternative model specifications that would make this possible are currently being tested. Even so, given the temporal grain of the time bins (500 years throughout the Holocene, except for the last 700 years, 100–350 years), we expect that, within uncertainty, the majority of sample ages will not shift among time bins. While REVEALS does quantify standard errors associated with relative abundance estimates, these standard errors are not considered by the REVEALS-GMRF approach. This means that uncertainty estimates from the REVEALS-GMRF approach quantify the uncertainty determined by the variability in REVEALS fractional land cover around the estimated spatial field (Fig. S4). Validation experiments would be useful to understand the impacts of sample unevenness; such experiments have been done using the REVEALS-GMRF approach for Europe (Pirzamanbein et al., 2018). This work generally showed little change in the predictions when data were withheld. These cross-validation experiments have a high computational burden. Future work aims to improve computational efficiency of the approach, at which point such experiments will be possible for larger domains like North America.

To address these limitations with the REVEALS workflow (spatial and temporal incompleteness, input parameter uncertainty, and uncertainty quantification), other forms of PVMs have been developed. ROPES uses pollen accumulation rates and REVEALS to estimate pollen productivity (Theuerkauf and Couwenberg, 2018). However, the dependence of ROPES on pollen accumulation rates may limit its widespread utility. At many sites, pollen accumulation rates have high uncertainties due to variations in sedimentation rate, few radiometric dates and poor chronological controls, and spike counting uncertainties (Perrotti et al., 2022). STEPPS is a Bayesian spatiotemporal PVM (Dawson et al., 2016, 2019). While theoretically sound, STEPPS is computationally intensive, and its estimates are dependent upon the density and quality of spatial forest compositional calibration datasets, limiting its applicability to continental-scale domains. Other spatial Bayesian models developed for high-resolution networks of pollen and vegetation data suggest that if the spatial site density is too low, STEPPS and simi-

larly structured PVMs can overestimate pollen dispersal distance (Liu et al., 2022).

4.4 Future work

With North American REVEALS-based reconstructions now in place, all middle and high latitudes in the Northern Hemisphere have quantitative reconstructions of Holocene land cover that are well constrained by dense networks of fossil pollen records (Githumbi et al., 2022b; Li et al., 2023). The reconstructions for North America and Europe also have estimates of uncertainty from the spatiotemporal GMRF model (Pirzamanbein et al., 2018). This hemispheric coverage now enables the creation of a next generation of modeling scenarios, well constrained by data, to explore land cover feedbacks in the Holocene climate system (Harrison et al., 2020), with relevance to both the Holocene temperature conundrum (Kaufman and Broadman, 2023; Liu et al., 2014) and the question of the missing Holocene carbon source (Brovkin et al., 2019; Indermühle et al., 1999; Ruddiman, 2003). These land cover reconstructions also help identify places where new local-scale, site-based research is needed to better understand human impacts, better constrain land cover changes in areas of sparse data and high uncertainty, and better understand how local and taxon-level dynamics scale up to affect regional- to continental-scale vegetation and climate dynamics.

Multiple opportunities exist to further enhance these reconstructions. Firstly, this work underscores the critical need for more work to better constrain PPEs and fall speeds, particularly for North American plant taxa. The REVEALS estimates in this analysis appear to be particularly sensitive to the parameterizations for under-represented taxa such as *Abies* and *Acer*. Secondly, these land cover reconstructions could be further parsed into boreal, temperate, and subtropical components, given what is known about these individual pollen types and their climatic affinities. However, statistically modeling more finely resolved land cover groupings or taxa is complicated by the many zero-count observations in more finely resolved groupings, especially for such a large spatiotemporal domain (Haslett et al., 2021). Thirdly, these pollen-based vegetation reconstructions would be improved by the incorporation of additional proxies, particularly in semi-arid regions, where carbon isotopic records from soils, lakes, speleothems, and other archives can provide information about the relative abundance of C_3 and C_4 grasslands (Braun et al., 2019; Nordt et al., 2007) and phytoliths can provide information about grassland composition (Blinnikov et al., 2002; Evett and Bartolome, 2013), although multiple factors affect $\delta^{13}C$ variations (Fohlmeister et al., 2020). Fourthly, for some subregions where a dense network of high-resolution, well-dated records exists, such as New England (Oswald et al., 2018).

Lastly, given the maturation of pollen–vegetation modeling as a field of study and the emergence of multiple PVMs, there is now the opportunity for intercomparison studies among PVMs and, perhaps, the development of ensemble-based inferences of past vegetation cover. There is a long history of methodological comparisons in pollen-based paleoclimatic inferences and paleoclimatology more broadly (Chevalier et al., 2020). Few systematic intercomparisons of PVMs yet exist (Roberts et al., 2018), although individual papers have discussed strengths and weaknesses of different modeling approaches (Liu et al., 2022; Theuerkauf et al., 2012). Initial efforts are underway to compare land cover reconstructions from REVEALS-GMRF to those from the Bayesian spatiotemporal model STEPPS. Moreover, given that ensemble-based approaches have been shown to have higher predictive ability in fields such as climate modeling and species distribution modeling (Deser et al., 2020; Bothe et al., 2013; Naimi and Araújo, 2016; Thuiller et al., 2009), there is value in developing approaches for ensemble-based PVMs for past land cover inference.

5 Conclusions

Continental-scale changes in land cover in North America during the Holocene are the outcome of multiple interacting drivers operating over a range of temporal and spatial scales. For much of the Holocene (ca. 8 to 1.5 ka), the spatial configurations of continental-scale fractional forest cover were broadly stable. Major continental-scale trends included early Holocene afforestation, a middle Holocene peak in the areal proportion of summergreen trees and shrubs, and a last-millennium increase in open land. These trends were driven by taxon-level dynamics that varied strongly within and among regions. The regional dynamics can be attributed to individualistic postglacial shifts in the range and abundance of plant taxa driven by changing climates and increased land area after deglaciation; abrupt and large species-level events, such as the mid-Holocene collapse of eastern hemlock; and a shift from localized land use during the late Holocene to massive ecosystem transformation following Euro-American settlement. This work rejects the ideas of both pre-industrial forest stability and widespread major conversions in land cover type.

This work contributes to the LandCover6k initiative to produce continental- to global-scale reconstructions of Holocene land cover dynamics that are well constrained by proxy data and are quantified using consistent methods. These REVEALS-GMRF reconstructions establish realistic benchmark scenarios constraining and assimilating with Earth system model simulations of the interactions among Holocene climate, land cover, and anthropogenic change. In addition, they can help refine Holocene models of land use and land cover change, provide a foundation for comparisons among PVMs, and indicate priority areas for future new site-level research. Scaling up from these continental to hemispheric and global products will enable further testing

of hypotheses about the drivers and feedbacks of Holocene land cover change, both biogeophysical and biogeochemical. These reconstructions also highlight several potentially important but unstudied vegetation–atmosphere feedbacks, including the collapse of eastern hemlock at ca. 5 ka and a positive feedback loop between mid-Holocene peaks in seasonality of insolation, temperature, and vegetation phenology.

Comparison of the REVEALS-GMRF land cover reconstructions with those inferred from alternate PVMs is a research priority. REVEALS-GMRF depends on a suite of input variables that are both uncertain and exhibit spatial and temporal variation not accounted for in the model. Also, the use of a post-hoc Bayesian GMRF interpolation step means that uncertainty of reconstructions associated with these assumptions is not fully characterized.

Finally, this work emphasizes the importance of quantifying ecosystem processes and feedbacks between the land surface and climate system. Holocene land cover changes in North America are non-negligible, and there is a pressing need to refine ecosystem models, in particular when those models are coupled within an Earth system model. The availability of well-constrained data products has been a major barrier to this effort. Paleoecology and palynology are reaching a new level of maturity with respect to advances in data discovery and accessibility, along with development of consistent analytical methods that permit interpretability of large-scale spatiotemporal change. Data assimilation experiments that integrate these reconstructions into Earth system models have the potential to resolve major questions in the field, such as the Holocene temperature conundrum and disentangling the effects of climate–vegetation–human interactions upon Holocene vegetation and climate dynamics.

Code and data availability. Code and data used in this workflow are publicly available at https://github.com/andydawson/reveals-na (last access: 10 October 2025; DOI: https://doi.org/10.5281/zenodo.17309166, Dawson, 2025). The land cover reconstructions from both REVEALS and REVEALS-GMRF are archived on Dryad at https://doi.org/10.5061/dryad.c2fqz61m5 (Dawson et al., 2025). The description and implementation of the digitization of lake area is available at https://github.com/NeotomaDB/neotoma_lakes (last access: 10 October 2025; DOI: https://doi.org/10.5281/zenodo.10535435, Goring, 2024).

Supplement. The supplement related to this article is available online at https://doi.org/10.5194/cp-21-2031-2025-supplement.

Author contributions. AD and JWW co-designed and co-wrote the paper, with AD leading on REVEALS analyses and figure generation. MJG helped initiate this effort, led PAGES LandCover6k, and coordinated activities with other continental-scale mapping groups. BP and JL assisted with the GMRF modeling and analyses, while SJG assisted with Neotoma data provision and digitization of lake size. RSA, AB, DF, KG, DGG, TL, TAM, WO, BS, and CW all contributed new records to the North American Pollen Database in Neotoma and assisted in data interpretation. All authors contributed to article development and revision.

Competing interests. The contact author has declared that none of the authors has any competing interests.

Disclaimer. Publisher's note: Copernicus Publications remains neutral with regard to jurisdictional claims made in the text, published maps, institutional affiliations, or any other geographical representation in this paper. While Copernicus Publications makes every effort to include appropriate place names, the final responsibility lies with the authors.

Special issue statement. This article is part of the special issue "Past vegetation dynamics and their role in past climate changes". It is not associated with a conference.

Acknowledgements. We acknowledge the support, community, and leadership of the Past Global Change (PAGES) project and the LandCover6k working group (https://pastglobalchanges.org/science/wg/former/landcover6k/intro, last access: 22 September 2025). Data were obtained from the Neotoma Paleoecology Database (http://www.neotomadb.org, last access: 22 September 2025) and its constituent database, the North American Pollen Database. The work of data contributors, data stewards, and the Neotoma community is gratefully acknowledged. Digitization of basin areas was assisted by Jenna Kilsevich, Grace Roper, Claire Rubbelke, Grace Tunski, Mathias Trachsel, and Bailey Zak.

Financial support. The Past Global Change (PAGES) project working group, LandCover6k (https://pastglobalchanges.org/science/wg/former/landcover6k/intro, last access: 22 September 2025), received support from the Swiss National Science Foundation, the Swiss Academy of Sciences, the US National Science Foundation, and the Chinese Academy of Sciences. This work is also supported through an NSERC Discovery Grant to Andria Dawson. Marie-José Gaillard received support from the Swedish Strategic Research Area (SRA) ModElling the Regional and Global Earth system (MERGE); http://www.merge.lu.se (last access: 22 September 2025). Support for Neotoma is from the NSF Geoinformatics program (grant no. 1948926).

Review statement. This paper was edited by Thomas Hickler and reviewed by Jed Kaplan and one anonymous referee.

References

Abraham, V., Oušková, V., and Kuneš, P.: Present-day vegetation helps quantifying past land cover in selected regions of the Czech Republic, PLoS One, 9, e100117, https://doi.org/10.1371/journal.pone.0100117, 2014.

Alder, J. R. and Hostetler, S. W.: Global climate simulations at 3000-year intervals for the last 21 000 years with the GENMOM coupled atmosphere–ocean model, Clim. Past, 11, 449–471, https://doi.org/10.5194/cp-11-449-2015, 2015.

Alessandri, A., Catalano, F., De Felice, M., Van den Hurk, B., and Balsamo, G.: Varying snow and vegetation signatures of surface-albedo feedback on the Northern Hemisphere land warming, Environ. Res. Lett., 16, 034023, https://doi.org/10.1088/1748-9326/abd65f, 2021.

Allison, T. D., Moeller, R. E., and Davis, M. B.: Pollen in laminated sediments provides evidence of mid-Holocene forest pathogen outbreak, Ecology, 67, 1101–1105, https://doi.org/10.2307/1939835, 1986.

Alt, M., McWethy, D. B., Everett, R., and Whitlock, C.: Millennial scale climate-fire-vegetation interactions in a mid-elevation mixed coniferous forest, Mission Range, northwestern Montana, USA, Quaternary Res., 90, 66–82, https://doi.org/10.1017/qua.2018.25, 2018.

Anderson, L. L., Hu, F. S., Nelson, D. M., Petit, R. J., and Paige, K. N.: Ice-age endurance: DNA evidence of a white spruce refugium in Alaska, P. Natl. Acad. Sci. USA, 103, 12447–12450, https://doi.org/10.1073/pnas.0605310103, 2006.

Anderson, P. M. and Brubaker, L. B.: Vegetation history of northcentral Alaska: A mapped summary of late-Quaternary pollen data, Quaternary Sci. Rev., 13, 71–92, https://doi.org/10.1016/0277-3791(94)90125-2, 1994.

Anderson, R. S.: Postglacial biogeography of Sierra lodgepole pine (*Pinus contorta* var. *murrayana*) in California, Écoscience, 3, 343–351, https://doi.org/10.1080/11956860.1996.11682352, 1996.

Anderson, R. S. and Carpenter, S. L.: Vegetation change in Yosemite Valley, Yosemite National Park, California, during the protohistoric period, Madroño, 38, 1–13, https://www.jstor.org/stable/41424832 (last access: 10 October 2025), 1991.

Anderson, R. S., Davis, R. B., Miller, N. G., and Stuckenrath, Jr., R.: History of late- and post-glacial vegetation and disturbance around Upper South Branch Pond, northern Maine, Can. J. Bot., 64, 1977–1986, https://doi.org/10.1139/b86-262, 1986.

Anderson, R. S., Allen, C. D., Toney, J. L., Jass, R. B., and Bair, A. N.: Holocene vegetation and fire regimes in subalpine and mixed conifer forests, southern Rocky Mountains, USA, Int. J. Wildland Fire, 17, 96–114, https://doi.org/10.1071/WF07028, 2008.

Anderson, R. S., Kaufman, D. S., Berg, E., Schiff, C., and Daigle, T.: Holocene biogeography of *Tsuga mertensiana* and other conifers in the Kenai Mountains and Prince William Sound, south-central Alaska, Holocene, 27, 485–495, https://doi.org/10.1177/0959683616670217, 2017.

Anderson, R. S., Berg, E., Williams, C., and Clark, T.: Postglacial vegetation community change over an elevational gradient on the western Kenai Peninsula, Alaska: pollen records from Sunken Island and Choquette Lakes, J. Quaternary Sci., 34, 309–322, https://doi.org/10.1002/jqs.3102, 2019.

Azuara, J., Mazier, F., Lebreton, V., Sugita, S., Viovy, N., and Combourieu-Nebout, N.: Extending the applicability of the REVEALS model for pollen-based vegetation reconstructions to coastal lagoons, Holocene, 29, 1109–1112, https://doi.org/10.1177/0959683619838024, 2019.

Bartlein, P. J., Hostletler, S. W., and Alder, J. R.: Paleoclimate, in: Climate Change in North America, Springer International Publishing, 1–51, https://doi.org/10.1007/978-3-319-03768-4_1, 2014.

Bhiry, N. and Filion, L.: Mid-Holocene hemlock decline in eastern North America linked with phytophagous insect activity, Quaternary Res., 45, 312–320, https://doi.org/10.1006/qres.1996.0032, 1996.

Black, B. A., Ruffner, C. M., and Abrams, M. D.: Native American influences on the forest composition of the Allegheny Plateau, northwest Pennsylvania, Can. J. Forest Res., 36, 1266–1275, https://doi.org/10.1139/x06-027, 2006.

Blarquez, O. and Aleman, J. C.: Tree biomass reconstruction shows no lag in postglacial afforestation of eastern Canada, Can. J. Forest Res., 46, 485–498, https://doi.org/10.1139/cjfr-2015-0201, 2015.

Blinnikov, M., Busacca, A., and Whitlock, C.: Reconstruction of the late Pleistocene grassland of the Columbia basin, Washington, USA, based on phytolith records in loess, Palaeogeogr. Palaeocl., 177, 77–101, https://doi.org/10.1016/S0031-0182(01)00353-4, 2002.

Bodmer, H.: Über den windpollen, Nat. Tech., 3, 294–298, 1922.

Bonan, G.: Ecological climatology: concepts and applications, Cambridge University Press, https://doi.org/10.1017/CBO9781107339200, 2015.

Bonan, G. B. and Doney, S. C.: Climate, ecosystems, and planetary futures: The challenge to predict life in Earth system models, Science, 359, eaam8328, https://doi.org/10.1126/science.aam8328, 2018.

Booth, R. K., Brewer, S., Blaauw, M., Minckley, T. A., and Jackson, S. T.: Decomposing the mid-Holocene *Tsuga* decline in eastern North America, Ecology, 93, 1841–1852, https://doi.org/10.1890/11-2062.1, 2012.

Bothe, O., Jungclaus, J. H., Zanchettin, D., and Zorita, E.: Climate of the last millennium: ensemble consistency of simulations and reconstructions, Clim. Past, 9, 1089–1110, https://doi.org/10.5194/cp-9-1089-2013, 2013.

Bradshaw, R. H. W. and Webb, I., T.: Relationships between contemporary pollen and vegetation data from Wisconsin and Michigan, USA, Ecology, 66, 721–737, https://doi.org/10.2307/1940533, 1985.

Braun, K., Bar-Matthews, M., Matthews, A., Ayalon, A., Cowling, R. M., Karkanas, P., Fisher, E. C., Dyez, K., Zilberman, T., and Marean, C. W.: Late Pleistocene records of speleothem stable isotopic compositions from Pinnacle Point on the South African south coast, Quaternary Res., 91, 265–288, https://doi.org/10.1017/qua.2018.61, 2019.

Briles, C. E., Whitlock, C., Bartlein, P. J., and Higuera, P.: Regional and local controls on postglacial vegetation and fire in the Siskiyou Mountains, northern California, USA, Palaeogeogr. Palaeocl., 265, 159–169, https://doi.org/10.1016/j.palaeo.2008.05.007, 2008.

Broström, A., Nielsen, A. B., Gaillard, M.-J., Hjelle, K., Mazier, F., Binney, H., Bunting, J., Fyfe, R., Meltsov, V., and Poska,

A.: Pollen productivity estimates of key European plant taxa for quantitative reconstruction of past vegetation: a review, Veg. Hist. Archaeobot., 17, 461–478, https://doi.org/10.1007/s00334-008-0148-8, 2008.

Brovkin, V., Raddatz, T., Reick, C. H., Claussen, M., and Gayler, V.: Global biogeophysical interactions between forest and climate, Geophys. Res. Lett., 36, https://doi.org/10.1029/2009GL037543, 2009.

Brovkin, V., Lorenz, S., Raddatz, T., Ilyina, T., Stemmler, I., Toohey, M., and Claussen, M.: What was the source of the atmospheric CO_2 increase during the Holocene?, Biogeosciences, 16, 2543–2555, https://doi.org/10.5194/bg-16-2543-2019, 2019.

Brugam, R. B. and Swain, P.: Diatom indicators of peatland development at Pogonia Bog Pond, Minnesota, USA, Holocene, 10, 453–464, https://doi.org/10.1191/095968300668251084, 2000.

Brugger, S. O. and Rhode, D.: Impact of Pleistocene–Holocene climate shifts on vegetation and fire dynamics and its implications for Prearchaic humans in the central Great Basin, USA, J. Quaternary Sci., 35, 987–993, https://doi.org/10.1002/jqs.3248, 2020.

Calder, W. J. and Shuman, B. N.: Extensive wildfires, climate change, and an abrupt state change in subalpine ribbon forests, Colorado, Ecology, 98, 2585–2600, https://doi.org/10.1002/ecy.1959, 2017.

Chandan, D. and Peltier, W. R.: African Humid Period precipitation sustained by robust vegetation, soil, and lake feedbacks, Geophys. Res. Lett., 47, e2020GL088728, https://doi.org/10.1029/2020GL088728, 2020.

Chaput, M. A. and Gajewski, K.: Relative pollen productivity estimates and changes in Holocene vegetation cover in the deciduous forest of southeastern Quebec, Canada, Botany, 96, 299–317, https://doi.org/10.1139/cjb-2017-0193, 2018.

Chen, J., Zhang, Q., Huang, W., Lu, Z., Zhang, Z., and Chen, F.: Northwestward shift of the northern boundary of the East Asian summer monsoon during the mid-Holocene caused by orbital forcing and vegetation feedbacks, Quaternary Sci. Rev., 268, 107136, https://doi.org/10.1016/j.quascirev.2021.107136, 2021.

Chen, L. and Dirmeyer, P. A.: Adapting observationally based metrics of biogeophysical feedbacks from land cover/land use change to climate modeling, Environ. Res. Lett., 11, 034002, https://doi.org/10.1088/1748-9326/11/3/034002, 2016.

Chevalier, M., Davis, B. A. S., Heiri, O., Seppä, H., Chase, B. M., Gajewski, K., Lacourse, T., Telford, R. J., Finsinger, W., Guiot, J., Kühl, N., Maezumi, S. Y., Tipton, J. R., Carter, V. A., Brussel, T., Phelps, L. N., Dawson, A., Zanon, M., Vallé, F., Nolan, C., Mauri, A., de Vernal, A., Izumi, K., Holmström, L., Marsicek, J., Goring, S., Sommer, P. S., Chaput, M., and Kupriyanov, D.: Pollen-based climate reconstruction techniques for late Quaternary studies, Earth-Sci. Rev., 210, 103384, https://doi.org/10.1016/j.earscirev.2020.103384, 2020.

Clark, J. S., Hussey, T., and Royall, P. D.: Presettlement analogs for Quaternary fire regimes in eastern North America, J. Paleolimnol., 16, 79–96, https://doi.org/10.1007/BF00173273, 1996.

Cruz-Silva, E., Harrison, S. P., Marinova, E., and Prentice, I. C.: A new method based on surface-sample pollen data for reconstructing palaeovegetation patterns, J. Biogeogr., 49, 1381–1396, https://doi.org/10.1111/jbi.14448, 2022.

Cwynar, L. C. and Spear, R. W.: Paleovegetation and paleoclimatic changes in the Yukon at 6 ka BP, Geogr. Phys. Quatern., 49, 29–35, https://doi.org/10.7202/033027ar, 1995.

Dallmeyer, A., Kleinen, T., Claussen, M., Weitzel, N., Cao, X., and Herzschuh, U.: The deglacial forest conundrum, Nat. Commun., 13, 6035, https://doi.org/10.1038/s41467-022-33646-6, 2022.

Dallmeyer, A., Poska, A., Marquer, L., Seim, A., and Gaillard, M.-J.: The challenge of comparing pollen-based quantitative vegetation reconstructions with outputs from vegetation models – a European perspective, Clim. Past, 19, 1531–1557, https://doi.org/10.5194/cp-19-1531-2023, 2023.

Dalton, A. S., Margold, M., Stokes, C. R., Tarasov, L., Dyke, A. S., Adams, R. S., Allard, S., Arends, H. E., Atkinson, N., Attig, J. W., Barnett, P. J., Barnett, R. L., Batterson, M., Bernatchez, P., Borns, H. W., Breckenridge, A., Briner, J. P., Brouard, E., Campbell, J. E., Carlson, A. E., Clague, J. J., Curry, B. B., Daigneault, R.-A., Dubé-Loubert, H., Easterbrook, D. J., Franzi, D. A., Friedrich, H. G., Funder, S., Gauthier, M. S., Gowan, A. S., Harris, K. L., Hétu, B., Hooyer, T. S., Jennings, C. E., Johnson, M. D., Kehew, A. E., Kelley, S. E., Kerr, D., King, E. L., Kjeldsen, K. K., Knaeble, A. R., Lajeunesse, P., Lakeman, T. R., Lamothe, M., Larson, P., Lavoie, M., Loope, H. M., Lowell, T. V., Lusardi, B. A., Manz, L., McMartin, I., Nixon, F. C., Occhietti, S., Parkhill, M. A., Piper, D. J. W., Pronk, A. G., Richard, P. J. H., Ridge, J. C., Ross, M., Roy, M., Seaman, A., Shaw, J., Stea, R. R., Teller, J. T., Thompson, W. B., Thorleifson, L. H., Utting, D. J., Veillette, J. J., Ward, B. C., Weddle, T. K., and Wright, H. E.: An updated radiocarbon-based ice margin chronology for the last deglaciation of the North American Ice Sheet Complex, Quaternary Sci. Rev., 234, 106223, https://doi.org/10.1016/j.quascirev.2020.106223, 2020.

Davis, M. B.: Pollen evidence of changing land use around the shores of Lake Washington, Northwest Sci., 47, 133–148, https://hdl.handle.net/11299/178248, 1973.

Davis, M. B.: Outbreaks of forest pathogens in Quaternary history, in: Proceedings of the Fourth International Palynological Conference, Lucknow, India, 216–227, https://hdl.handle.net/11299/178237, 1981.

Davis, M. B.: Palynology after Y2K–understanding the source area of pollen in sediments, Annu. Rev. Earth Pl. Sc., 28, 1–18, https://doi.org/10.1146/annurev.earth.28.1.1, 2000.

Dawson, A.: andydawson/REVEALS-NA: REVEALS-NA-CP (Version v1), Zenodo [code and data set], https://doi.org/10.5281/zenodo.17309166, 2025.

Dawson, A., Paciorek, C. J., McLachlan, J. S., Goring, S., Williams, J. W., and Jackson, S. T.: Quantifying pollen-vegetation relationships to reconstruct ancient forests using 19th-century forest composition and pollen data, Quaternary Sci. Rev., 137, 156–175, https://doi.org/10.1016/j.quascirev.2016.01.012, 2016.

Dawson, A., Cao, X., Chaput, M., Hopla, E., Li, F., Edwards, M., Fyfe, R., Gajewski, K., Goring, S., Herzschuh, U., and others: Finding the magnitude of human-induced Northern Hemisphere land-cover transformation between 6 and 0.2 ka BP, PAGES Mag., 26, 34–35, https://doi.org/10.22498/pages.26.1.34, 2018.

Dawson, A., Paciorek, C. J., Goring, S., Jackson, S., McLachlan, J., and Williams, J. W.: Quantifying trends and uncertainty in prehistoric forest composition in the upper Midwestern United States, Ecology, 100, e02856, https://doi.org/10.1002/ecy.2856, 2019.

Dawson, A., Williams, J., Goring, S., Gaillard, M.-J., Pirzamanbein, B., Lindstrom, J., Anderson, R. S., Brunelle, A., Foster, D., Gajewski, K., Gavin, D. G., Lacourse, T., Minckley, T. A., Oswald, W., Shuman, B., and Whitlock, C.: North America Holocene land cover: REVEALS-GMRF, Dryad [data set], https://doi.org/10.5061/dryad.c2fqz61m5, 2025.

Dean, W. E., Bradbury, J. P., Anderson, R. Y., and Barnosky, C. W.: The variability of Holocene climate change: Evidence from varved lake sediments, Science, 226, 1191–1194, https://doi.org/10.1126/science.226.4679.1191, 1984.

Delcourt, H. R. and Delcourt, P. A.: Postglacial rise and decline of *Ostrya virginiana* (Mill) K Koch and *Carpinus caroliniana* Walt in eastern North-America: Predictable responses of forest species to cyclic changes in seasonality of climates, J. Biogeogr., 21, 137–150, https://doi.org/10.2307/2845468, 1994.

Delcourt, P. A., Delcourt, H. R., Cridlebaugh, P. A., and Chapman, J.: Holocene ethnobotanical and paleoecological record of human impact on vegetation in the Little Tennessee River Valley, Tennessee, Quaternary Res., 25, 330–349, https://doi.org/10.1016/0033-5894(86)90005-0, 1986.

Deser, C., Lehner, F., Rodgers, K. B., Ault, T., Delworth, T. L., DiNezio, P. N., Fiore, A., Frankignoul, C., Fyfe, J. C., Horton, D. E., Kay, J. E., Knutti, R., Lovenduski, N. S., Marotzke, J., McKinnon, K. A., Minobe, S., Randerson, J., Screen, J. A., Simpson, I. R., and Ting, M.: Insights from Earth system model initial-condition large ensembles and future prospects, Nat. Clim. Change, 10, 277–286, https://doi.org/10.1038/s41558-020-0731-2, 2020.

Dyke, A. and Prest, V.: Late Wisconsinan and Holocene History of the Laurentide Ice Sheet, Geogr. Phys. Quatern., 41, 237–263, https://doi.org/10.7202/032681ar, 1987.

Edwards, M. E., Brubaker, L. B., Lozhkin, A. V., and Anderson, P. M.: Structurally novel biomes: a response to past warming in Beringia, Ecology, 86, 1696–1703, https://doi.org/10.1890/03-0787, 2005.

Ellis, E. C.: Land use and ecological change: A 12,000-Year History, Annu. Rev. Environ. Resour., 46, 1–33, https://doi.org/10.1146/annurev-environ-012220-010822, 2021.

Evans, M. N., Tolwinski-Ward, S. E., Thompson, D. M., and Anchukaitis, K. J.: Applications of proxy system modeling in high resolution paleoclimatology, Quaternary Sci. Rev., 76, 16–28, https://doi.org/10.1016/j.quascirev.2013.05.024, 2013.

Evett, R. R. and Bartolome, J. W.: Phytolith evidence for the extent and nature of prehistoric Californian grasslands, Holocene, 23, 1644–1649, https://doi.org/10.1177/0959683613499056, 2013.

Faison, E. K., Foster, D. R., Oswald, W. W., Hansen, B. C. S., and Doughty, E.: Early Holocene openlands in southern New England, Ecology, 87, 2537–2547, https://doi.org/10.1890/0012-9658(2006)87[2537:EHOISN]2.0.CO;2, 2006.

Finkelstein, S. A., Gajewski, K., and Viau, A. E.: Improved resolution of pollen taxonomy allows better biogeographical interpretation of post-glacial forest development: analyses from the North American Pollen Database, J. Ecol., 94, 415–430, https://doi.org/10.1111/j.1365-2745.2005.01087.x, 2006.

Flantua, S. G. A., Mottl, O., Felde, V. A., Bhatta, K. P., Birks, H. H., Grytnes, J.-A., Seddon, A. W. R., and Birks, H. J. B.: A guide to the processing and standardization of global palaeoecological data for large-scale syntheses using fossil pollen, Global Ecol. Biogeogr., 32, 1377–1394, https://doi.org/10.1111/geb.13693, 2023.

Fohlmeister, J., Voarintsoa, N. R. G., Lechleitner, F. A., Boyd, M., Brandtstätter, S., Jacobson, M. J., and Oster, J. L.: Main controls on the stable carbon isotope composition of speleothems, Geochim. Cosmochim. Ac., 279, 67–87, https://doi.org/10.1016/j.gca.2020.03.042, 2020.

Foley, J. A., Kutzbach, J. E., Coe, M. T., and Levis, S.: Feedbacks between climate and boreal forests during the Holocene epoch, Nature, 371, 52–54, https://doi.org/10.1038/371052a0, 1994.

Foster, D. R. and Aber, J. D.: Forests in Time: The Environmental Consequences of 1000 Years of Change in New England, Yale University Press, https://doi.org/10.1017/S0022050704313124, 2004.

Foster, D. R., Oswald, W. W., Faison, E. K., Doughty, E. D., and Hansen, B. C. S.: A climatic driver for abrupt mid-Holocene vegetation dynamics and the hemlock decline in New England, Ecology, 87, 2959–2966, https://doi.org/10.1890/0012-9658(2006)87[2959:ACDFAM]2.0.CO;2, 2006.

Fréchette, B., Richard, P. J. H., Grondin, P., Lavoie, M., and Larouche, A. C.: Histoire postglaciaire de la végétation et du climat des pessières et des sapinières de l'ouest du Québec, Mém. Rech. For., 179, https://mrnf.gouv.qc.ca//documents/forets/recherche/Memoire179.pdf (last access: 22 October 2025), 2018.

Fréchette, B., Richard, P. J. H., Lavoie, M., Grondin, P., and Larouche, A. C.: Histoire postglaciaire de la végétation et du climat des pessières et des sapinières de l'est du Québec et du Labrador méridional, Mém. Rech. For., 186, 170 pp., https://mrnf.gouv.qc.ca//documents/forets/recherche/MRF186.pdf (last access: 22 October 2025), 2021.

Fyfe, R., Roberts, N., and Woodbridge, J.: A pollen-based pseudobiomisation approach to anthropogenic land-cover change, Holocene, 20, 1165–1171, https://doi.org/10.1177/0959683610369509, 2010.

Gaillard, M., Whitehouse, N., Madella, M., Morrison, K., and von Gunten, L.: Past land use and land cover, PAGES Mag., 26, 1–44, https://doi.org/10.22498/pages.26.1, 2018.

Gaillard, M. J. and LandCover6k Steering Group: LandCover6k: Global anthropogenic land-cover change and its role in past climate, PAGES Mag., 23, 38–39, https://doi.org/10.22498/pages.23.1.38, 2015.

Gaillard, M.-J., Sugita, S., Mazier, F., Trondman, A.-K., Broström, A., Hickler, T., Kaplan, J. O., Kjellström, E., Kokfelt, U., Kuneš, P., Lemmen, C., Miller, P., Olofsson, J., Poska, A., Rundgren, M., Smith, B., Strandberg, G., Fyfe, R., Nielsen, A. B., Alenius, T., Balakauskas, L., Barnekow, L., Birks, H. J. B., Bjune, A., Björkman, L., Giesecke, T., Hjelle, K., Kalnina, L., Kangur, M., van der Knaap, W. O., Koff, T., Lageräs, P., Latałowa, M., Leydet, M., Lechterbeck, J., Lindbladh, M., Odgaard, B., Peglar, S., Segerström, U., von Stedingk, H., and Seppä, H.: Holocene land-cover reconstructions for studies on land cover-climate feedbacks, Clim. Past, 6, 483–499, https://doi.org/10.5194/cp-6-483-2010, 2010.

Gajewski, K.: Environmental history of the northwestern Québec Treeline, Quaternary Sci. Rev., 206, 29–43, https://doi.org/10.1016/j.quascirev.2018.12.025, 2019.

Gajewski, K., Kriesche, B., Chaput, M. A., Kulik, R., and Schmidt, V.: Human–vegetation interactions during the Holocene

in North America, Veg. Hist. Archaeobot., 28, 635–647, https://doi.org/10.1007/s00334-019-00721-w, 2019.

Gajewski, K., Grenier, A., and Payette, S.: Climate, fire and vegetation history at treeline east of Hudson Bay, northern Québec, Quaternary Sci. Rev., 254, 106794, https://doi.org/10.1016/j.quascirev.2021.106794, 2021.

Gavin, D. G. and Brubaker, L. B.: Late Pleistocene and Holocene Environmental Change on the Olympic Peninsula, Washington, Springer, https://doi.org/10.1007/978-3-319-11014-1, 2014.

Gavin, D. G., Brubaker, L. B., and Greenwald, D. N.: Postglacial climate and fire-mediated vegetation change on the western Olympic Peninsula, Washington (USA), Ecol. Monogr., 83, 471–489, https://doi.org/10.1890/12-1742.1, 2013.

Gavin, D. G., White, A., Sanborn, P. T., and Hebda, R. J.: Deglacial landforms and Holocene vegetation trajectories in the northern interior cedar-hemlock forests of British Columbia, in: Untangling the Quaternary Period—A Legacy of Stephen C. Porter, vol. 548, edited by: Waitt, R. B., Thackray, G. D., and Gillespie, A. R., Geological Society of America, https://doi.org/10.1130/2020.2548(05), 2021.

George, A., Widell, S., Goring, S. J., Roth, R. E., and Williams, J. W.: Range Mapper: An adaptable process for making and using interactive, animated web maps of late-Quaternary open paleoecological data, Open Quat., 9, 15, https://doi.org/10.5334/oq.114, 2023.

Githumbi, E., Fyfe, R., Gaillard, M.-J., Trondman, A.-K., Mazier, F., Nielsen, A.-B., Poska, A., Sugita, S., Woodbridge, J., Azuara, J., Feurdean, A., Grindean, R., Lebreton, V., Marquer, L., Nebout-Combourieu, N., Stančikaitė, M., Tanţău, I., Tonkov, S., Shumilovskikh, L., and LandClimII data contributors: European pollen-based REVEALS land-cover reconstructions for the Holocene: methodology, mapping and potentials, Earth Syst. Sci. Data, 14, 1581–1619, https://doi.org/10.5194/essd-14-1581-2022, 2022a.

Githumbi, E., Pirzamanbein, B., Lindström, J., Poska, A., Fyfe, R., Mazier, F., Nielsen, A. B., Sugita, S., Trondman, A.-K., Woodbridge, J., and others: Pollen-based maps of past regional vegetation cover in Europe over 12 Millennia–evaluation and potential, Front. Ecol. Evol., 10, 795794, https://doi.org/10.3389/fevo.2022.795794, 2022b.

Giuliano, C. and Lacourse, T.: Holocene fire regimes, fire-related plant functional types, and climate in south-coastal British Columbia forests, Ecosphere, 14, e4416, https://doi.org/10.1002/ecs2.4416, 2023.

Goring, S.: Neotoma Lakes Assignment (Version 0.1), Zenodo [software], https://doi.org/10.5281/zenodo.10535435, 2024.

Grimm, E. C., Bradshaw, R. H. W., Giesecke, T., Lézine, A.-M., Takahara, H., and Williams, J. W.: Pollen databases and their application, in: Encyclopaedia of Quaternary Sciences, edited by: Elias, S. A., https://hal.science/hal-01491073 (last access: 22 October 2025), 2013.

Gugger, P. F. and Sugita, S.: Glacial populations and post-glacial migration of Douglas-fir based on fossil pollen and macrofossil evidence, Quaternary Sci. Rev., 29, 2052–2070, https://doi.org/10.1016/j.quascirev.2010.04.022, 2010.

Guo, Z., Zhou, X., and Wu, H.: Glacial-interglacial water cycle, global monsoon and atmospheric methane changes, Clim. Dynam., 39, 1073–1092, https://doi.org/10.1007/s00382-011-1147-5, 2012.

Haas, J. N. and McAndrews, J. H.: The summer drought related hemlock (*Tsuga canadensis*) decline in eastern North America 5,700 to 5,100 years ago, Symposium on Sustainable Management of Hemlock Ecosystems in Eastern North America, Durham, New Hampshire, USA, 22–24 June 1999, 81–88, https://research.fs.usda.gov/treesearch/4141 (last access: 22 October 2025), 1999.

Hansen, B. C. S. and Engstrom, D. R.: Vegetation history of Pleasant Island, southeastern Alaska, since 13,000 yr B.P., Quaternary Res., 46, 161–175, https://doi.org/10.1006/qres.1996.0056, 1996.

Harrison, S. P., Gaillard, M.-J., Stocker, B. D., Vander Linden, M., Klein Goldewijk, K., Boles, O., Braconnot, P., Dawson, A., Fluet-Chouinard, E., Kaplan, J. O., Kastner, T., Pausata, F. S. R., Robinson, E., Whitehouse, N. J., Madella, M., and Morrison, K. D.: Development and testing scenarios for implementing land use and land cover changes during the Holocene in Earth system model experiments, Geosci. Model Dev., 13, 805–824, https://doi.org/10.5194/gmd-13-805-2020, 2020.

Haslett, J., Parnell, A. C., Hinde, and de Andrade Moral: Modelling Excess Zeros in Count Data: A New Perspective on Modelling Approaches – Haslett – 2022 – International Statistical Review – Wiley Online Library, 90, 216–236, https://doi.org/10.1111/insr.12479, 2021.

Hayashi, R., Sasaki, N., Takahara, H., Sugita, S., and Saito, H.: Estimation of absolute pollen productivity based on the flower counting approach: A review, Quatern. Int., 641, 122–137, https://doi.org/10.1016/j.quaint.2022.04.015, 2022.

Hellman, S., Gaillard, M.-J., Broström, A., and Sugita, S.: The REVEALS model, a new tool to estimate past regional plant abundance from pollen data in large lakes: validation in southern Sweden, J. Quaternary Sci., 23, 21–42, https://doi.org/10.1002/jqs.1126, 2008a.

Hellman, S. E., Gaillard, M., Broström, A., and Sugita, S.: Effects of the sampling design and selection of parameter values on pollen-based quantitative reconstructions of regional vegetation: a case study in southern Sweden using the REVEALS model, Veg. Hist. Archaeobot., 17, 445–459, https://doi.org/10.1007/s00334-008-0149-7, 2008b.

Herzschuh, U.: Legacy of the Last Glacial on the present-day distribution of deciduous versus evergreen boreal forests, Glob. Ecol. Biogeogr., 29, 198–206, https://doi.org/10.1111/geb.13018, 2020.

Herzschuh, U., Böhmer, T., Li, C., Chevalier, M., Hébert, R., Dallmeyer, A., Cao, X., Bigelow, N. H., Nazarova, L., Novenko, E. Y., Park, J., Peyron, O., Rudaya, N. A., Schlütz, F., Shumilovskikh, L. S., Tarasov, P. E., Wang, Y., Wen, R., Xu, Q., and Zheng, Z.: LegacyClimate 1.0: a dataset of pollen-based climate reconstructions from 2594 Northern Hemisphere sites covering the last 30 kyr and beyond, Earth Syst. Sci. Data, 15, 2235–2258, https://doi.org/10.5194/essd-15-2235-2023, 2023.

Hoevers, R., Broothaerts, N., and Verstraeten, G.: The potential of REVEALS-based vegetation reconstructions using pollen records from alluvial floodplains, Veg. Hist. Archaeobot., 31, 525–540, https://doi.org/10.1007/s00334-022-00866-1, 2022.

Hollinger, D. Y., Ollinger, S. V., Richardson, A. D., Meyers, T. P., Dail, D. B., Martin, M. E., Scott, N. A., Arkebauer, T. J., Baldocchi, D. D., and Clark, K. L.: Albedo estimates for land surface models and support for a new paradigm based on fo-

liage nitrogen concentration, Glob. Change Biol., 16, 696–710, https://doi.org/10.1111/j.1365-2486.2009.02028.x, 2010.

Huybers, P.: Early Pleistocene glacial cycles and the integrated summer insolation forcing, Science, 313, 508–511, https://doi.org/10.1126/science.1125249, 2006.

Iglesias, V. and Whitlock, C.: If the trees burn, is the forest lost? Past dynamics in temperate forests help inform management strategies, Philos. T. Roy. Soc. B, 375, 20190115, https://doi.org/10.1098/rstb.2019.0115, 2020.

Iglesias, V., Whitlock, C., Krause, T. R., and Baker, R. G.: Past vegetation dynamics in the Yellowstone region highlight the vulnerability of mountain systems to climate change, J. Biogeogr., 45, 1768–1780, https://doi.org/10.1111/jbi.13364, 2018.

Indermühle, A., Stocker, T. F., Joos, F., Fischer, H., Smith, H. J., Wahlen, M., Deck, B., Mastroianni, D., Tschumi, J., Blunier, T., Meyer, R., and Stauffer, B.: Holocene carbon-cycle dynamics based on CO_2 trapped in ice at Taylor Dome, Antarctica, Nature, 398, 121–126, https://doi.org/10.1038/18158, 1999.

Ireland, A. W. and Booth, R. K.: Hydroclimatic variability drives episodic expansion of a floating peat mat in a North American kettlehole basin, Ecology, 92, 11–18, https://doi.org/10.1890/10-0770.1, 2010.

Islebe, G. A., Hooghiemstra, H., Brenner, M., Curtis, J. H., and Hodell, D. A.: A Holocene vegetation history from lowland Guatemala, Holocene, 6, 265–271, https://doi.org/10.1177/095968369600600302, 1996.

Jackson, S. T.: Pollen source area and representation in small lakes of the northeastern United States, Rev. Palaeobot. Palynol., 63, 53–76, https://doi.org/10.1016/0034-6667(90)90006-5, 1990.

Jackson, S. T. and Lyford, M. E.: Pollen dispersal models in Quaternary plant ecology: Assumptions, parameters, and prescriptions, Bot. Rev., 65, 39–75, https://doi.org/10.1007/BF02856557, 1999.

Jackson, S. T. and Whitehead, D. R.: Holocene vegetation patterns in the Adirondack Mountains, Ecology, 72, 641–654, https://doi.org/10.2307/2937204, 1991.

Jackson, S. T., Overpeck, J. T., Webb, I., T., Keattch, S. E., and Anderson, K. H.: Mapped plant-macrofossil and pollen records of late Quaternary vegetation change in eastern North America, Quaternary Sci. Rev., 16, 1–70, https://doi.org/10.1016/S0277-3791(96)00047-9, 1997.

Jackson, S. T., Betancourt, J. L., Booth, R. K., and Gray, S. T.: Ecology and the ratchet of events: Climate variability, niche dimensions, and species distributions, P. Natl. Acad. Sci. USA, 106, 19685–19692, https://doi.org/10.1073/pnas.0901644106, 2009.

Jensen, A. M., Fastovich, D., Watson, B. I., Gill, J. L., Jackson, S. T., Russell, J. M., Bevington, J., Hayes, K., Lininger, K., Rubbelke, C., Schellinger, G. C., and Williams, J. W.: More than one way to kill a spruce forest: The role of fire and climate in the late-glacial termination of spruce woodlands across the southern Great Lakes, J. Ecol., 109, 459–477, https://doi.org/10.1111/1365-2745.13517, 2021.

Kaplan, J. O., Krumhardt, K. M., and Zimmermann, N.: The prehistoric and preindustrial deforestation of Europe, Quaternary Sci. Rev., 28, 3016–3034, https://doi.org/Doi 10.1016/J.Quascirev.2009.09.028, 2009.

Kaplan, J. O., Krumhardt, K. M., Gaillard, M.-J., Sugita, S., Trondman, A.-K., Fyfe, R., Marquer, L., Mazier, F., and Nielsen, A. B.: Constraining the deforestation history of Europe: Evaluation of historical land use scenarios with pollen-based land cover reconstructions, Land, 6, 91, https://doi.org/10.3390/land6040091, 2017.

Kaufman, D. S. and Broadman, E.: Revisiting the Holocene global temperature conundrum, Nature, 614, 425–435, https://doi.org/10.1038/s41586-022-05536-w, 2023.

Kelly, R., Chipman, M. L., Higuera, P. E., Stefanova, I., Brubaker, L. B., and Hu, F. S.: Recent burning of boreal forests exceeds fire regime limits of the past 10,000 years, P. Natl. Acad. Sci. USA, 110, 13055–13060, https://doi.org/10.1073/pnas.1305069110, 2013.

Klein Goldewijk, K., Beusen, A., and Janssen, P.: Long-term dynamic modeling of global population and built-up area in a spatially explicit way: HYDE 3.1, Holocene, 20, 565–573, https://doi.org/10.1177/0959683609356587, 2010.

Klein Goldewijk, K., Beusen, A., van Drecht, G., and de Vos, M.: The HYDE 3.1 spatially explicit database of human-induced global land-use change over the past 12,000 years, Global Ecol. Biogeogr., 20, 73–86, https://doi.org/10.1111/j.1466-8238.2010.00587.x, 2011.

Knight, C. A., Anderson, L., Bunting, M. J., Champagne, M., Clayburn, R. M., Crawford, J. N., Klimaszewski-Patterson, A., Knapp, E. E., Lake, F. K., Mensing, S. A., Wahl, D., Wanket, J., Watts-Tobin, A., Potts, M. D., and Battles, J. J.: Land management explains major trends in forest structure and composition over the last millennium in California's Klamath Mountains, P. Natl. Acad. Sci. USA, 119, e2116264119, https://doi.org/10.1073/pnas.2116264119, 2022.

Kuparinen, A., Markkanen, T., Riikonen, H., and Vesala, T.: Modeling air-mediated dispersal of spores, pollen and seeds in forested areas, Ecol. Model., 208, 177–188, https://doi.org/10.1016/j.ecolmodel.2007.05.023, 2007.

Kutzbach, Bartlein, P. J., Foley, J. A., Harrison, S. P., Hostetler, S. W., Liu, Z., Prentice, I. C., and Webb III, T.: Potential role of vegetation feedback in the climate sensitivity of high-latitude regions: A case study at 6000 years B.P., Global Biogeochem. Cy., 10, 727–736, https://doi.org/10.1029/96GB02690, 1996.

Lacourse, T.: Environmental change controls postglacial forest dynamics through interspecific differences in life-history traits, Ecology, 90, 2149–2160, https://doi.org/10.1890/08-1136.1, 2009.

Lacourse, T. and Adeleye, M. A.: Climate and species traits drive changes in Holocene forest composition along an elevation gradient in Pacific Canada, Front. Ecol. Evol., 10, 838545, https://doi.org/10.3389/fevo.2022.838545, 2022.

Lacourse, T. and Gajewski, K.: Current practices in building and reporting age-depth models, Quaternary Res., 96, 28–38, https://doi.org/10.1017/qua.2020.47, 2020.

Lacourse, T., Mathewes, R. W., and Hebda, R. J.: Paleoecological analyses of lake sediments reveal prehistoric human impact on forests at Anthony Island UNESCO World Heritage Site, Queen Charlotte Islands (Haida Gwaii), Canada, Quaternary Res., 68, 177–183, https://doi.org/10.1016/j.yqres.2007.04.005, 2007.

Lacourse, T., Delepine, J. M., Hoffman, E. H., and Mathewes, R. W.: A 14,000 year vegetation history of a hypermaritime island on the outer Pacific coast of Canada based on fossil pollen, spores and conifer stomata, Quaternary Res., 78, 572–582, https://doi.org/10.1016/j.yqres.2012.08.008, 2012.

Leopold, E. B. and Boyd, R.: An ecological history of old prairie areas, southwestern Washington, in: Indians, Fire and the Land, edited by: Boyd, R., Oregon State University Press, https://doi.org/10.1353/book94487, 139–166, 1999.

Lewis, S. L. and Maslin, M. A.: Defining the Anthropocene, Nature, 519, 171–180, https://doi.org/10.1038/nature14258, 2015.

Li, F., Gaillard, M.-J., Cao, X., Herzschuh, U., Sugita, S., Tarasov, P. E., Wagner, M., Xu, Q., Ni, J., and Wang, W.: Towards quantification of Holocene anthropogenic land-cover change in temperate China: A review in the light of pollen-based REVEALS reconstructions of regional plant cover, Earth-Sci. Rev., 203, 103119, https://doi.org/10.1016/j.earscirev.2020.103119, 2020.

Li, F., Gaillard, M.-J., Cao, X., Herzschuh, U., Sugita, S., Ni, J., Zhao, Y., An, C., Huang, X., Li, Y., Liu, H., Sun, A., and Yao, Y.: Gridded pollen-based Holocene regional plant cover in temperate and northern subtropical China suitable for climate modelling, Earth Syst. Sci. Data, 15, 95–112, https://doi.org/10.5194/essd-15-95-2023, 2023.

Liefert, D. T. and Shuman, B. N.: Pervasive desiccation of North American lakes during the late Quaternary, Geophys. Res. Lett., 47, e2019GL086412, https://doi.org/10.1029/2019GL086412, 2020.

Lindgren, F., Rue, H., and Lindström, J.: An explicit link between Gaussian fields and Gaussian Markov random fields: the stochastic partial differential equation approach, J. Roy. Stat. Soc. B, 73, 423–498, https://doi.org/10.1111/j.1467-9868.2011.00777.x, 2011.

Liu, Y., Ogle, K., Lichstein, J. W., and Jackson, S. T.: Estimation of pollen productivity and dispersal: How pollen assemblages in small lakes represent vegetation, Ecol. Monogr., 92, e1513, https://doi.org/10.1002/ecm.1513, 2022.

Liu, Z., Zhu, J., Rosenthal, Y., Zhang, X., Otto-Bliesner, B. L., Timmermann, A., Smith, R. S., Lohmann, G., Zheng, W., and Elison Timm, O.: The Holocene temperature conundrum, P. Natl. Acad. Sci. USA, 111, E3501–E3505, https://doi.org/10.1073/pnas.1407229111, 2014.

Loisel, J., van Bellen, S., Pelletier, L., Talbot, J., Hugelius, G., Karran, D., Yu, Z., Nichols, J., and Holmquist, J.: Insights and issues with estimating northern peatland carbon stocks and fluxes since the Last Glacial Maximum, Earth-Sci. Rev., 165, 59–80, https://doi.org/10.1016/j.earscirev.2016.12.001, 2017.

Long, C. J., Whitlock, C., Bartlein, P. J., and Millspaugh, S. H.: A 9000-year fire history from the Oregon Coast Range, based on a high-resolution charcoal study, Can. J. Forest Res., 28, 774–787, https://doi.org/10.1139/x98-051, 1998.

Long, C. J., Whitlock, C., and Bartlein, P. J.: Holocene vegetation and fire history of the Coast Range, western Oregon, USA, Holocene, 17, 917–926, https://doi.org/10.1177/0959683607082408, 2007.

Loranty, M. M., Berner, L. T., Goetz, S. J., Jin, Y., and Randerson, J. T.: Vegetation controls on northern high latitude snow-albedo feedback: observations and CMIP 5 model simulations, Glob. Change Biol., 20, 594–606, https://doi.org/10.1111/gcb.12391, 2014.

MacDonald, G. M.: Postglacial palaeoecology of the subalpine forest-grassland ecotone of southwestern Alberta: new insights on vegetation and climate change in the Canadian Rocky Mountains and adjacent foothills, Palaeogeogr. Palaeocl., 73, 155–173, https://doi.org/10.1016/0031-0182(89)90001-1, 1989.

MacDonald, G. M. and Cwynar, L. C.: Post-glacial population growth rates of Pinus contorta ssp. latifolia in western Canada, J. Ecol., 79, 417–429, https://doi.org/10.2307/2260723, 1991.

Marcott, S. A., Shakun, J. D., Clark, P. U., and Mix, A. C.: A reconstruction of regional and global temperature for the past 11,300 years, Science, 339, 1198–1201, https://doi.org/10.1126/science.1228026, 2013.

Marlon, J. R., Bartlein, P. J., Gavin, D. G., Long, C. J., Anderson, R. S., Briles, C. E., Brown, K. J., Colombaroli, D., Hallett, D. J., and Power, M. J.: Long-term perspective on wildfires in the western USA, P. Natl. Acad. Sci. USA, 109, E535–E543, https://doi.org/10.1073/pnas.1112839109, 2012.

Marsicek, J., Shuman, B. N., Bartlein, P. J., Shafer, S. L., and Brewer, S.: Reconciling divergent trends and millennial variations in Holocene temperatures, Nature, 554, 92–96, https://doi.org/10.1038/nature25464, 2018.

McAndrews, J. H. and Turton, C. L.: Canada geese dispersed cultigen pollen grains from prehistoric Iroquoian fields to Crawford Lake, Ontario, Canada, Palynology, 31, 9–18, https://doi.org/10.2113/gspalynol.31.1.9, 2007.

McKay, N. P., Emile-Geay, J., and Khider, D.: geoChronR – an R package to model, analyze, and visualize age-uncertain data, Geochronology, 3, 149–169, https://doi.org/10.5194/gchron-3-149-2021, 2021.

McMichael, C. N. H.: Ecological legacies of past human activities in Amazonian forests, New Phytol., 229, 2492–2496, https://doi.org/10.1111/nph.16888, 2020.

Mensing, S., Smith, J., Burkle Norman, K., and Allan, M.: Extended drought in the Great Basin of western North America in the last two millennia reconstructed from pollen records, 22nd Pac. Clim. Workshop, 188, 79–89, https://doi.org/10.1016/j.quaint.2007.06.009, 2008.

Minckley, T. A., Whitlock, C., and Bartlein, P. J.: Vegetation, fire, and climate history of the northwestern Great Basin during the last 14,000 years, Quaternary Sci. Rev., 26, 2167–2184, https://doi.org/10.1016/j.quascirev.2007.04.009, 2007.

Mottl, O., Flantua, S. G. A., Bhatta, K. P., Felde, V. A., Giesecke, T., Goring, S., Grimm, E. C., Haberle, S., Hooghiemstra, H., Ivory, S., Kuneš, P., Wolters, S., Seddon, A. W. R., and Williams, J. W.: Global acceleration in rates of vegetation change over the last 18,000 years, Science, 321, 860–864, https://doi.org/10.1126/science.abg1685, 2021.

Munoz, S. E. and Gajewski, K.: Distinguishing prehistoric human influence on late-Holocene forests in southern Ontario, Canada, Holocene, 20, 967–981, https://doi.org/10.1177/0959683610362815, 2010.

Munoz, S. E., Schroeder, S., Fike, D. A., and Williams, J. W.: A record of sustained prehistoric and historic land use from the Cahokia region, Illinois, USA, Geology, 42, 499–502, https://doi.org/10.1130/G35541.1, 2014.

Naimi, B. and Araújo, M. B.: sdm: a reproducible and extensible R platform for species distribution modelling, Ecography, 39, 368–375, 2016.

Napier, J. D. and Chipman, M. L.: Emerging palaeoecological frameworks for elucidating plant dynamics in response to fire and other disturbance, Global Ecol. Biogeogr., 31, 138–154, https://doi.org/10.1111/geb.13416, 2021.

Natural Resources Canada: National Hydro Network, Natural Resources Canada [data set], https://open.canada.ca/data/en/

dataset/a4b190fe-e090-4e6d-881e-b87956c07977 (last access: 22 October 2025), 2022.

Nelson, D. M., Hu, F. S., Grimm, E. C., Curry, B. B., and Slate, J. E.: The influence of aridity and fire on Holocene prairie communities in the eastern Prairie Peninsula, Ecology, 87, 2523–2536, https://doi.org/10.1890/0012-9658(2006)87[2523:TIOAAF]2.0.CO;2, 2006.

Niklas, K. J.: The motion of windborne pollen grains around conifer ovulate cones: implications on wind pollination, Am. J. Bot., 71, 356–374, https://doi.org/10.1002/j.1537-2197.1984.tb12523.x, 1984.

Nordt, L., von Fischer, J., and Tieszen, L.: Late Quaternary temperature record from buried soils of the North American Great Plains, Geology, 35, 159–162, https://doi.org/10.1130/G23345A.1, 2007.

Oswald, W. W. and Foster, D. R.: Middle-Holocene dynamics of *Tsuga canadensis* (eastern hemlock) in northern New England, USA, Holocene, 22, 71–78, https://doi.org/10.1177/0959683611409774, 2012.

Oswald, W. W., Doughty, E. D., Foster, D. R., Shuman, B. N., and Wagner, D. L.: Evaluating the role of insects in the middle-Holocene *Tsuga* decline, J. Torrey Bot. Soc., 144, 35–39, https://doi.org/10.3159/TORREY-D-15-00074.1, 2017.

Oswald, W. W., Foster, D., Shuman, B., Doughty, E., Faison, E. K., Hall, B., Hansen, B. C. S., Lindbladh, M., Marroquin, A., and Truebe, S.: Subregional variability in the response of New England vegetation to postglacial climate change, J. Biogeogr., 45, 2375–2388, https://doi.org/10.1111/jbi.13407, 2018.

Oswald, W. W., Foster, D. R., Shuman, B. N., Chilton, E. S., Doucette, D. L., and Duranleau, D. L.: Conservation implications of limited Native American impacts in pre-contact New England, Nat. Sustain., 3, 241–246, https://doi.org/10.1038/s41893-019-0466-0, 2020.

Otto, J., Raddatz, T., and Claussen, M.: Strength of forest-albedo feedback in mid-Holocene climate simulations, Clim. Past, 7, 1027–1039, https://doi.org/10.5194/cp-7-1027-2011, 2011.

Paciorek, C. J., Goring, S. J., Thurman, A., Cogbill, C. V., Williams, J. W., Mladenoff, D. J., Peters, J. A., Zhu, J., and McLachlan, J. S.: Statistically-estimated tree composition for the northeastern United States at the time of Euro-American settlement, PLoS One, 11, e0150087, https://doi.org/10.1371/journal.pone.0150087, 2016.

PALSEA (PALeo SEA level working group): The sea-level conundrum: case studies from palaeo-archives, J. Quaternary Sci., 25 19–25, https://doi.org/10.1002/jqs.1270, 2010.

Parnell, A. C., Haslett, J., Allen, J. R., Buck, C. E., and Huntley, B.: A flexible approach to assessing synchroneity of past events using Bayesian reconstructions of sedimentation history, Quaternary Sci. Rev., 27, 1872–1885, https://doi.org/10.1016/j.quascirev.2008.07.009, 2008.

Payette, S.: A paleo-perspective on ecosystem collapse in boreal North America, edited by: Canadell, J. G. and Jackson, R. B., Ecosyst. Collapse Clim. Change, 101–129, https://doi.org/10.1007/978-3-030-71330-0_5, 2021.

Payette, S., Filion, L., and Delwaide, A.: Spatially explicit fire-climate history of the boreal forest-tundra (eastern Canada) over the last 2000 years, Philos. Trans. Biol. Sci., 363, 2301–2316, https://doi.org/10.1098/rstb.2007.2201, 2008.

Payette, S., Couillard, P.-L., Frégeau, M., Laflamme, J., and Lavoie, M.: The velocity of postglacial migration of fire-adapted boreal tree species in eastern North America, P. Natl. Acad. Sci. USA, 119, e2210496119, https://doi.org/10.1073/pnas.2210496119, 2022.

Peltier, W. R.: Ice Age Paleotopography, Science, 265, 195–201, https://doi.org/10.1126/science.265.5169.195, 1994.

Peros, M. C., Gajewski, K., and Viau, A. E.: Continental-scale tree population response to rapid climate change, competition and disturbance, Global Ecol. Biogeogr., 17, 658–669, https://doi.org/10.1111/j.1466-8238.2008.00406.x, 2008.

Peros, M. C., Munoz, S. E., Gajewski, K., and Viau, A. E.: Prehistoric demography of North America inferred from radiocarbon data, J. Archaeol. Sci., 37, 656–664, https://doi.org/10.1016/j.jas.2009.10.029, 2010.

Perrotti, A. G., Ramiadantsoa, T., O'Keefe, J., and Nuñez Otaño, N.: Uncertainty in coprophilous fungal spore concentration estimates, Front. Ecol. Evol., 10, https://doi.org/10.3389/fevo.2022.1086109, 2022.

Pirzamanbein, B., Lindström, J., Poska, A., Sugita, S., Trondman, A.-K., Fyfe, R., Mazier, F., Nielsen, A. B., Kaplan, J. O., Bjune, A., Birks, H. J. B., Giesecke, T., Kangur, M., Latałowa, M., Marquer, L., Smith, B., and Gaillard, M.-J.: Creating spatially continuous maps of past land cover from point estimates: A new statistical approach applied to pollen data, Ecol. Complex., 20, 127–141, https://doi.org/10.1016/j.ecocom.2014.09.005, 2014.

Pirzamanbein, B., Lindström, J., Poska, A., and Gaillard, M.-J.: Modelling spatial compositional data: Reconstructions of past land cover and uncertainties, Spat. Stat., 24, 14–31, https://doi.org/10.1016/j.spasta.2018.03.005, 2018.

Pirzamanbein, B., Poska, A., and Lindström, J.: Bayesian reconstruction of past land cover from pollen data: Model robustness and sensitivity to auxiliary variables, Earth Space Sci., 7, e2018EA00057, https://doi.org/10.1029/2018EA000547, 2020.

Pongratz, J., Reick, C. H., Raddatz, T., and Claussen, M.: Biogeophysical versus biogeochemical climate response to historical anthropogenic land cover change, Geophys. Res. Lett., 37, L08702, https://doi.org/10.1029/2010GL043010, 2010.

Prentice, I. C.: Pollen representation, source area, and basin size: toward a unified theory of pollen analysis, Quaternary Res., 23, 76–86, https://doi.org/10.1016/0033-5894(85)90073-0, 1985.

Prentice, I. C., Jolly, D., and BIOME 6000 participants: Mid-Holocene and glacial-maximum vegetation geography of the northern continents and Africa, J. Biogeogr., 27, 507–519, https://doi.org/10.1046/j.1365-2699.2000.00425.x, 2000.

Prentice, I. C., Harrison, S. P., and Bartlein, P. J.: Global vegetation and terrestrial carbon cycle changes after the last ice age, New Phytol., 189, 988–998, https://doi.org/10.1111/j.1469-8137.2010.03620.x, 2011.

Raiho, A., Paciorek, C. J., Dawson, A., Jackson, S. T., Mladenoff, D. J., Williams, J. W., and McLachlan, J. S.: 8000-year doubling of Midwestern forest biomass driven by population- and biome-scale processes, Science, 376, 1491–1495, https://doi.org/10.1126/science.abk3126, 2022.

Reimer, P. J., Austin, W. E., Bard, E., Bayliss, A., Blackwell, P. G., Ramsey, C. B., Butzin, M., Cheng, H., Edwards, R. L., and Friedrich, M.: The IntCal20 Northern Hemisphere radiocarbon age calibration curve (0–55 cal kBP), Radiocarbon, 62, 725–757, https://doi.org/10.1017/RDC.2020.41, 2020.

Richard, P., Fréchette, B., Grondin, P., and Lavoie, M.: Histoire postglaciaire de la végétation de la forêt boréale du Québec et du Labrador, Nat. Can., 144, 63–76, https://doi.org/10.7202/1070086ar, 2020.

Roberts, N., Fyfe, R. M., Woodbridge, J., Gaillard, M. J., Davis, B. A. S., Kaplan, J. O., Marquer, L., Mazier, F., Nielsen, A. B., Sugita, S., Trondman, A. K., and Leydet, M.: Europe's lost forests: a pollen-based synthesis for the last 11,000 years, Sci. Rep., 8, 716, https://doi.org/10.1038/s41598-017-18646-7, 2018.

Rogelj, J., Popp, A., Calvin, K. V., Luderer, G., Emmerling, J., Gernaat, D., Fujimori, S., Strefler, J., Hasegawa, T., Marangoni, G., Krey, V., Kriegler, E., Riahi, K., van Vuuren, D. P., Doelman, J., Drouet, L., Edmonds, J., Fricko, O., Harmsen, M., Havlík, P., Humpenöder, F., Stehfest, E., and Tavoni, M.: Scenarios towards limiting global mean temperature increase below 1.5 ° C, Nat. Clim. Change, 8, 325–332, https://doi.org/10.1038/s41558-018-0091-3, 2018.

Roos, C. I.: Scale in the study of Indigenous burning, Nat. Sustain., 3, 898–899, https://doi.org/10.1038/s41893-020-0579-5, 2020.

Roos, C. I., Zedeño, M. N., Hollenback, K. L., and Erlick, M. M. H.: Indigenous impacts on North American Great Plains fire regimes of the past millennium, P. Natl. Acad. Sci. USA, 115, 8143–8148, https://doi.org/10.1073/pnas.1805259115, 2018.

Rosenberg, S. M., Walker, I. R., and Mathewes, R. W.: Postglacial spread of hemlock (Tsuga) and vegetation history in Mount Revelstoke National Park, British Columbia, Canada, Can. J. Bot., 81, 139–151, https://doi.org/10.1139/b03-015, 2003.

Ruddiman, W. F.: The anthropogenic greenhouse era began thousands of years ago, Clim. Change, 61, 261–293, https://doi.org/10.1023/B:CLIM.0000004577.17928.fa, 2003.

Ruddiman, W. F.: The Anthropocene, Annu. Rev. Earth Pl. Sc., 41, 4.1–4.24, https://doi.org/10.1146/annurev-earth-050212-123944, 2013.

Serge, M.-A., Mazier, F., Fyfe, R., Gaillard, M.-J., Klein, T., Lagnoux, A., Galop, D., Githumbi, E., Mindrescu, M., and Nielsen, A. B.: Testing the effect of relative pollen productivity on the REVEALS model: a validated reconstruction of Europe-wide holocene vegetation, Land, 12, 986, https://doi.org/10.3390/land12050986, 2023.

Shuman, B., Webb, T., III, Bartlein, P., and Williams, J. W.: The anatomy of a climatic oscillation: vegetation change in eastern North America during the Younger Dryas chronozone, Quaternary Sci. Rev., 21, 1777–1791, https://doi.org/10.1016/S0277-3791(02)00030-6, 2002.

Shuman, B. N. and Marsicek, J.: The structure of Holocene climate change in mid-latitude North America, Quaternary Sci. Rev., 141, 38–51, https://doi.org/10.1016/j.quascirev.2016.03.009, 2016.

Shuman, B. N., Newby, P. C., Huang, Y., and Webb, I., T.: Evidence for the close climatic control of New England vegetation history, Ecology, 85, 1297–1310, https://doi.org/10.1890/02-0286, 2004.

Shuman, B. N., Marsicek, J., Oswald, W. W., and Foster, D. R.: Predictable hydrological and ecological responses to Holocene North Atlantic variability, P. Natl. Acad. Sci. USA, 116, 5985–5990, https://doi.org/10.1073/pnas.1814307116, 2019.

Shuman, B. N., Stefanescu, I. C., Grigg, L. D., Foster, D. R., and Oswald, W. W.: A millennial-scale oscillation in latitudinal temperature gradients along the western North Atlantic during the mid-Holocene, Geophys. Res. Lett., 50, e2022GL102556, https://doi.org/10.1029/2022GL102556, 2023.

Sjögren, P., van der Knaap, W. O., Huusko, A., and van Leeuwen, J. F. N.: Pollen productivity, dispersal, and correction factors for major tree taxa in the Swiss Alps based on pollen-trap results, Rev. Palaeobot. Palyno., 152, 200–210, https://doi.org/10.1016/j.revpalbo.2008.05.003, 2008.

Snitker, G., Roos, C. I., Sullivan, A. P., Maezumi, S. Y., Bird, D. W., Coughlan, M. R., Derr, K. M., Gassaway, L., Klimaszewski-Patterson, A., and Loehman, R. A.: A collaborative agenda for archaeology and fire science, Nat. Ecol. Evol., 6, 835–839, https://doi.org/10.1038/s41559-022-01759-2, 2022.

Spear, R. W., Davis, M. B., and Shane, L. C. K.: Late Quaternary history of low- and mid-elevation vegetation in the White Mountains of New Hampshire, Ecol. Monogr., 64, 85–109, https://doi.org/10.2307/2937056, 1994.

Stegner, M. A. and Spanbauer, T. L.: North American pollen records provide evidence for macroscale ecological changes in the Anthropocene, P. Natl. Acad. Sci. USA, 120, e2306815120, https://doi.org/10.1073/pnas.2306815120, 2023.

Stephens, L., Fuller, D., Boivin, N., Rick, T., Gauthier, N., Kay, A., Marwick, B., Armstrong, C. G., Barton, C. M., Denham, T., Douglass, K., Driver, J., Janz, L., Roberts, P., Rogers, J. D., Thakar, H., Altaweel, M., Johnson, A. L., Sampietro Vattuone, M. M., Aldenderfer, M., Archila, S., Artioli, G., Bale, M. T., Beach, T., Borrell, F., Braje, T., Buckland, P. I., Jiménez Cano, N. G., Capriles, J. M., Diez Castillo, A., Çilingiroğlu, Ç., Negus Cleary, M., Conolly, J., Coutros, P. R., Covey, R. A., Cremaschi, M., Crowther, A., Der, L., di Lernia, S., Doershuk, J. F., Doolittle, W. E., Edwards, K. J., Erlandson, J. M., Evans, D., Fairbairn, A., Faulkner, P., Feinman, G., Fernandes, R., Fitzpatrick, S. M., Fyfe, R., Garcea, E., Goldstein, S., Goodman, R. C., Dalpoim Guedes, J., Herrmann, J., Hiscock, P., Hommel, P., Horsburgh, K. A., Hritz, C., Ives, J. W., Junno, A., Kahn, J. G., Kaufman, B., Kearns, C., Kidder, T. R., Lanoë, F., Lawrence, D., Lee, G.-A., Levin, M. J., Lindskoug, H. B., López-Sáez, J. A., Macrae, S., Marchant, R., Marston, J. M., McClure, S., McCoy, M. D., Miller, A. V., Morrison, M., Motuzaite Matuzeviciute, G., Müller, J., Nayak, A., Noerwidi, S., Peres, T. M., Peterson, C. E., Proctor, L., Randall, A. R., Renette, S., Robbins Schug, G., Ryzewski, K., Saini, R., Scheinsohn, V., Schmidt, P., Sebillaud, P., Seitsonen, O., Simpson, I. A., Sołtysiak, A., Speakman, R. J., Spengler, R. N., Steffen, M. L., et al.: Archaeological assessment reveals Earth's early transformation through land use, Science, 365, 897–902, https://doi.org/10.1126/science.aax1192, 2019.

Strandberg, G., Kjellström, E., Poska, A., Wagner, S., Gaillard, M.-J., Trondman, A.-K., Mauri, A., Davis, B. A. S., Kaplan, J. O., Birks, H. J. B., Bjune, A. E., Fyfe, R., Giesecke, T., Kalnina, L., Kangur, M., van der Knaap, W. O., Kokfelt, U., Kuneš, P., Latałowa, M., Marquer, L., Mazier, F., Nielsen, A. B., Smith, B., Seppä, H., and Sugita, S.: Regional climate model simulations for Europe at 6 and 0.2 k BP: sensitivity to changes in anthropogenic deforestation, Clim. Past, 10, 661–680, https://doi.org/10.5194/cp-10-661-2014, 2014.

Strandberg, G., Lindström, J., Poska, A., Zhang, Q., Fyfe, R., Githumbi, E., Kjellström, E., Mazier, F., Nielsen, A. B., Sugita, S., Trondman, A.-K., Woodbridge, J., and Gaillard, M.-J.: Mid-Holocene European climate revisited: New high-resolution regional climate model simulations using

pollen-based land-cover, Quaternary Sci. Rev., 281, 107431, https://doi.org/10.1016/j.quascirev.2022.107431, 2022.

Sugita, S.: Theory of quantitative reconstruction of vegetation I: pollen from large sites REVEALS regional vegetation composition, Holocene, 17, 229–241, https://doi.org/10.1177/0959683607075837, 2007a.

Sugita, S.: Theory of quantitative reconstruction of vegetation II: all you need is LOVE, Holocene, 17, 243–257, https://doi.org/10.1177/0959683607075838, 2007b.

Sugita, S., Parshall, T., Calcote, R., and Walker, K.: Testing the Landscape Reconstruction Algorithm for spatially explicit reconstruction of vegetation in northern Michigan and Wisconsin, Quaternary Res., 74, 289–300, https://doi.org/10.1016/j.yqres.2010.07.008, 2010.

Sutton, O. G.: Micrometeorology: A Study of Physical Processes in the Lowest Layers of the Earth's Atmosphere, McGraw-Hill, 333 pp., 1953.

Theuerkauf, M. and Couwenberg, J.: ROPES reveals past land cover and PPEs From single pollen records, Front. Earth Sci., 6, https://doi.org/10.3389/feart.2018.00014, 2018.

Theuerkauf, M., Kuparinen, A., and Joosten, H.: Pollen productivity estimates strongly depend on assumed pollen dispersal, Holocene, 23, 14–24, https://doi.org/10.1177/0959683612450194, 2012.

Theuerkauf, M., Couwenberg, J., Kuparinen, A., and Liebscher, V.: A matter of dispersal: REVEALSinR introduces state-of-the-art dispersal models to quantitative vegetation reconstruction, Veg. Hist. Archaeobot., 25, 541–553, https://doi.org/10.1007/s00334-016-0572-0, 2016.

Thompson, A. J., Zhu, J., Poulsen, C. J., Tierney, J. E., and Skinner, C. B.: Northern Hemisphere vegetation change drives a Holocene thermal maximum, Sci. Adv., 8, eabj6535, https://doi.org/10.1126/sciadv.abj6535, 2022.

Thompson, J. R., Carpenter, D. N., Cogbill, C. V., and Foster, D. R.: Four centuries of change in northeastern United States forests, PLoS One, 8, e72540, https://doi.org/10.1371/journal.pone.0072540, 2013.

Thompson, R. S.: Late Quaternary environments in Ruby Valley, Nevada, Quaternary Res., 37, 1–15, https://doi.org/10.1016/0033-5894(92)90002-Z, 1992.

Thompson, R. S., Anderson, K. H., and Bartlein, P. J.: Atlas of Relations Between Climatic Parameters and Distributions of Important Trees and Shrubs in North America–Introduction and Conifers, U.S. Department of the Interior, U.S. Geological Survey, https://doi.org/10.3133/pp1650AB, 1999.

Thuiller, W., Lafourcade, B., Engler, R., and Araújo, M. B.: BIOMOD – A platform for ensemble forecasting of species distributions, Ecography, 32, 369–373, https://doi.org/10.1111/j.1600-0587.2008.05742.x, 2009.

Trachsel, M. and Telford, R. J.: All age–depth models are wrong, but are getting better, Holocene, 27, 860–869, https://doi.org/10.1177/0959683616675939, 2017.

Trachsel, M., Dawson, A., Paciorek, C. J., Williams, J. W., McLachlan, J. S., Cogbill, C. V., Foster, D. R., Goring, S. J., Jackson, S. T., Oswald, W. W., and Shuman, B. M.: Comparison of settlement-era vegetation reconstructions for STEPPS and REVEALS pollen–vegetation models in the northeastern United States, Quaternary Res., 95, 23–42, https://doi.org/10.1017/qua.2019.81, 2020.

Trondman, A.-K., Gaillard, M.-J., Mazier, F., Sugita, S., Fyfe, R., Nielsen, A. B., Twiddle, C., Barratt, P., Birks, H. J. B., Bjune, A. E., Björkman, L., Broström, A., Caseldine, C., David, R., Dodson, J., Dörfler, W., Fischer, E., van Geel, B., Giesecke, T., Hultberg, T., Kalnina, L., Kangur, M., van der Knaap, P., Koff, T., Kuneš, P., Lagerås, P., Latałowa, M., Lechterbeck, J., Leroyer, C., Leydet, M., Lindbladh, M., Marquer, L., Mitchell, F. J. G., Odgaard, B. V., Peglar, S. M., Persson, T., Poska, A., Rösch, M., Seppä, H., Veski, S., and Wick, L.: Pollen-based quantitative reconstructions of Holocene regional vegetation cover (plant-functional types and land-cover types) in Europe suitable for climate modelling, Glob. Change Biol., 21, 676–697, https://doi.org/10.1111/gcb.12737, 2015.

Trondman, A.-K., Gaillard, M.-J., Sugita, S., Björkman, L., Greisman, A., Hultberg, T., Lagerås, P., Lindbladh, M., and Mazier, F.: Are pollen records from small sites appropriate for REVEALS model-based quantitative reconstructions of past regional vegetation? An empirical test in southern Sweden, Veg. Hist. Archaeobot., 25, 131–151, https://doi.org/10.1007/s00334-015-0536-9, 2016.

Umbanhowar Jr., C. E., Camill, P., Geiss, C. E., and Teed, R.: Asymmetric vegetation responses to mid-Holocene aridity at the prairie-forest ecotone in south-central Minnesota, Quaternary Res., 66, 53–66, https://doi.org/10.1016/j.yqres.2006.03.005, 2006.

United States Geological Survey: National Hydrography Dataset (NHD Model v2.3.1), United States Geological Survey [data set], https://www.usgs.gov/national-hydrography/national-hydrography-dataset (last access: 22 October 2025), 2022.

van Vuuren, D. P., Stehfest, E., Gernaat, D. E. H. J., Doelman, J. C., van den Berg, M., Harmsen, M., de Boer, H. S., Bouwman, L. F., Daioglou, V., Edelenbosch, O. Y., Girod, B., Kram, T., Lassaletta, L., Lucas, P. L., van Meijl, H., Müller, C., van Ruijven, B. J., van der Sluis, S., and Tabeau, A.: Energy, land-use and greenhouse gas emissions trajectories under a green growth paradigm, Glob. Environ. Change, 42, 237–250, https://doi.org/10.1016/j.gloenvcha.2016.05.008, 2017.

Walsh, M. K., Whitlock, C., and Bartlein, P. J.: A 14,300-year-long record of fire–vegetation–climate linkages at Battle Ground Lake, southwestern Washington, Quaternary Res., 70, 251–264, https://doi.org/10.1016/j.yqres.2008.05.002, 2008.

Walsh, M. K., Pearl, C. A., Whitlock, C., Bartlein, P. J., and Worona, M. A.: An 11 000-year-long record of fire and vegetation history at Beaver Lake, Oregon, central Willamette Valley, Quaternary Sci. Rev., 29, 1093–1106, https://doi.org/10.1016/j.quascirev.2010.02.011, 2010.

Walsh, M. K., Marlon, J. R., Goring, S. J., Brown, K. J., and Gavin, D. G.: A regional perspective on Holocene fire–climate–human interactions in the Pacific Northwest of North America, Ann. Assoc. Am. Geogr., 105, 1135–1157, https://doi.org/10.1080/00045608.2015.1064457, 2015.

Whitlock, C.: Vegetational and climatic history of the Pacific Northwest during the last 20,000 years: Implications for understanding present-day biodiversity, Northwest Environ. J., 8, 5–28, 1992.

Whitlock, C., Colombaroli, D., Conedera, M., and Tinner, W.: Land-use history as a guide for forest conservation and management, Conserv. Biol., 32, 84–97, https://doi.org/10.1111/cobi.12960, 2018.

Whitmore, J., Gajewski, K., Sawada, M., Williams, J., Shuman, B., Bartlein, P., Minckley, T., Viau, A., Webb, T., Shafer, S.,Anderson, P., and Brubaker, L.: Modern pollen data from North America and Greenland for multi-scale paleoenvironmental applications, Quaternary Sci. Rev., 24, 1828–1848, https://doi.org/10.1016/j.quascirev.2005.03.005, 2005.

Wieczorek, M. and Herzschuh, U.: Compilation of relative pollen productivity (RPP) estimates and taxonomically harmonised RPP datasets for single continents and Northern Hemisphere extratropics, Earth Syst. Sci. Data, 12, 3515–3528, https://doi.org/10.5194/essd-12-3515-2020, 2020.

Williams, J. W. and Jackson, S. T.: Novel climates, no-analog communities, and ecological surprises, Front. Ecol. Environ., 5, 475–482, https://doi.org/10.1890/070037, 2007.

Williams, J. W., Shuman, B. N., and Webb, I., T.: Dissimilarity analyses of late-Quaternary vegetation and climate in eastern North America, Ecology, 82, 3346–3362, https://doi.org/10.1890/0012-9658(2001)082[3346:DAOLQV]2.0.CO;2, 2001.

Williams, J. W., Shuman, B. N., Webb, T., III, Bartlein, P. J., and Luduc, P. L.: Late-Quaternary vegetation dynamics in North America: scaling from taxa to biomes, Ecol. Monogr., 74, 309–334, https://doi.org/10.1890/02-4045, 2004.

Williams, J. W., Shuman, B., and Bartlein, P. J.: Rapid responses of the Midwestern prairie-forest ecotone to early Holocene aridity, Global Planet. Change, 66, 195–207, https://doi.org/10.1016/j.gloplacha.2008.10.012, 2009a.

Williams, J. W., Shuman, B., and Bartlein, P. J.: Rapid responses of the prairie-forest ecotone to early Holocene aridity in mid-continental North America, Global Planet. Change, 66, 195–207, https://doi.org/10.1016/j.gloplacha.2008.10.012, 2009b.

Williams, J. W., Tarasov, P., Brewer, S., and Notaro, M.: Late Quaternary variations in tree cover at the northern forest-tundra ecotone, J. Geophys. Res.-Biogeo., 116, G01017, https://doi.org/10.1029/2010JG001458, 2011a.

Williams, J. W., Tarasov, P. A., Brewer, S., and Notaro, M.: Late-Quaternary variations in tree cover at the northern forest-tundra ecotone, J. Geophys. Res.-Biogeo., 116, G01017, https://doi.org/10.1029/2010JG001458, 2011b.

Williams, J. W., Grimm, E. G., Blois, J., Charles, D. F., Davis, E., Goring, S. J., Graham, R., Smith, A. J., Anderson, M., Arroyo-Cabrales, J., Ashworth, A. C., Betancourt, J. L., Bills, B. W., Booth, R. K., Buckland, P., Curry, B., Giesecke, T., Hausmann, S., Jackson, S. T., Latorre, C., Nichols, J., Purdum, T., Roth, R. E., Stryker, M., and Takahara, H.: The Neotoma Paleoecology Database: A multi-proxy, international community-curated data resource, Quaternary Res., 89, 156–177, https://doi.org/10.1017/qua.2017.105, 2018.

Worona, M. A. and Whitlock, C.: Late Quaternary vegetation and climate history near Little Lake, central Coast Range, Oregon, Geol. Soc. Am. Bull., 107, 867–876, https://doi.org/10.1130/0016-7606(1995)107<0867:LQVACH>2.3.CO;2, 1995.

Yu, Z. C.: Northern peatland carbon stocks and dynamics: a review, Biogeosciences, 9, 4071–4085, https://doi.org/10.5194/bg-9-4071-2012, 2012.

Zapolska, A., Serge, M. A., Mazier, F., Quiquet, A., Renssen, H., Vrac, M., Fyfe, R., and Roche, D. M.: More than agriculture: Analysing time-cumulative human impact on European land-cover of second half of the Holocene, Quaternary Sci. Rev., 314, 108227, https://doi.org/10.1016/j.quascirev.2023.108227, 2023.